

Thermodynamic Bubble Ansatz

Luis F. Alday, Davide Gaiotto and Juan Maldacena

*School of Natural Sciences, Institute for Advanced Study
Princeton, NJ 08540, USA*

Motivated by the computation of scattering amplitudes at strong coupling, we consider minimal area surfaces in AdS_5 which end on a null polygonal contour at the boundary. We map the classical problem of finding the surface into an $SU(4)$ Hitchin system. The polygon with six edges is the first non-trivial example. For this case, we write an integral equation which determines the area as a function of the shape of the polygon. The equations are identical to those of the Thermodynamics Bethe Ansatz. Moreover, the area is given by the free energy of this TBA system. The high temperature limit of the TBA system can be exactly solved. It leads to an explicit expression for a special class of hexagonal contours.

1. Introduction

In this paper we consider a geometrical problem involving minimal surfaces in AdS . We prescribe a polygonal contour on the AdS boundary and we consider a minimal surface which ends on this contour. We devise a method for computing the area of the surface as a function of the boundary contour.

It is a generalization of the problem of finding the shape of soap bubbles, or Plateau problem [1], to AdS space. In the 19th century the study of surface tension was interesting for what it could reveal about interfaces and the size of atoms. For us, the study of this AdS “soap bubbles” is interesting for what it could eventually teach us about their constituents, gluons, and their scattering for all values of the coupling. While this is our motivation, the computations in this paper will be restricted to classical geometry (or strong coupling).

1.1. Gauge theory motivation

Our main motivation for focusing on this problem comes from the study of Wilson loops or scattering amplitudes in $\mathcal{N} = 4$ super Yang Mills theory. These observables are interesting in general gauge theories and contain a wealth of dynamical information. Since planar $\mathcal{N} = 4$ super Yang Mills theory is integrable [2,3], one hopes to be able to compute them at all values of the coupling. At strong coupling they can be computed in terms of classical strings in AdS_5 [4]. The classical equations of motion for a string say that the area should be extremized. Thus, we end up studying minimal surfaces in AdS_5 space. This problem becomes tractable because it is classically integrable [5,3]. In fact, we will use its classical integrability to find equations that determine the area.

We hope that our classical analysis will be a useful starting point for solving the problem at all values of the coupling. In fact, the final classical problem has a structure that looks like the Y system for the Thermodynamic Bethe Ansatz.

For the computation of operator dimensions the solutions to the classical problem [6,7] were very useful for eventually determining the full quantum solution [8,9,10,11]. We hope that the same will be true for the computation of scattering amplitudes.

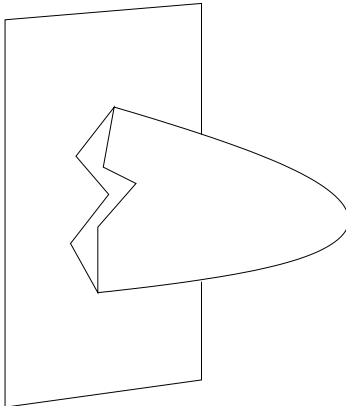


Fig. 1: We have a polygonal loop with null sides on the boundary of AdS . This polygon is denoted here by the jagged lines. We consider a minimal surface in the bulk that is ending on the polygon.

We consider surfaces that end at the AdS boundary on a special contour which is made out of null segments, see fig. 1. We are given a sequence of n points on the boundary, such that consecutive points are at a null distance, $x_{i,i+1}^2 = 0$. This defines a polygon with null sides. Conformal transformations act on this polygon and can change the positions of the points. One can define conformal invariant cross ratios which do not change under conformal transformations. These characterize the polygons up to conformal transformations. We will choose the points in such a way that the distance between all points which are not consecutive is spacelike. In this case, the minimal surface that ends on the contour is spacelike. It is a spacelike surface embedded in the Lorentzian signature AdS_5 space. Its area is infinite. This infinity is due to the IR divergencies of amplitudes or the UV divergencies of Wilson loops. One can define a renormalized area which is finite and conformal invariant. Our goal is to compute the renormalized area as a function of the cross ratios. In the context of scattering amplitudes, this quantity is called “remainder function”. See [12,13] for a perturbative, two loop evaluation of this function for six particles.

1.2. Outline of the method

The classical action for a string in AdS is conformal invariant. Thus, it contains a conserved holomorphic stress tensor $T(z)$, $\bar{T}(\bar{z})$ on the worldsheet. The Virasoro constraints are setting these to zero. In this case, we also have spin four holomorphic quantities $P(z)$, $\bar{P}(\bar{z})$. These are holomorphic and non-vanishing after we impose the equations of motion and the Virasoro constraints. These are additional local conserved quantities associated to the integrability of the theory. These currents play a crucial role in our method for

solving the problem. Via worldsheet conformal transformations $z \rightarrow w = f(z)$ we can locally set them to one $P(z) \rightarrow P(w) = 1$. This however, cannot be done globally without introducing some singularities. In our case the worldsheet can be parametrized by the whole complex plane and $P(z)$ is a polynomial. The degree of the polynomial determines the number of sides of the polygon. The coefficients of the polynomial (together with some extra parameters we will discuss later) encode the shape of the polygon .

The problem is integrable and it has a one parameter family of flat connections parametrized by a spectral parameter ζ . This family is encoding the infinite number of conserved non-local charges of the theory.

The flat connection goes to a constant at infinity and the solutions of the linear problem $(d + \mathcal{A})\psi = 0$ grow at infinity. The solutions of the linear problem, for $\zeta = 1$, encode the *AdS* coordinates and the fact that they go to infinity as $z \rightarrow \infty$ implies that they go to the boundary of *AdS*. They go to different points on the boundary of *AdS* in different angular sectors of the z plane. These sectors are called Stokes sectors. In any problem which has Stokes sectors we can define cross ratios, which end up being the same as the spacetime cross ratios when $\zeta = 1$.

The advantage of introducing the spectral parameter $\zeta \neq 1$ is that the problem of determining the cross ratios as a function of the polynomial coefficients simplifies when $\zeta \rightarrow 0$ or when $\zeta \rightarrow \infty$. In this limit we can determine the form of the cross ratios as a function of the coefficients of the polynomial $P(z)$. In addition, we expect that the cross ratios are analytic functions of ζ away from $\zeta = 0, \infty$. The cross ratios as a function of ζ display a sort of Stokes phenomenon as $\zeta \rightarrow 0, \infty$. One can define certain cross ratios which are analytic within certain angular sectors in the ζ -plane and have simple asymptotics for $\zeta \rightarrow 0, \infty$. When we change angular sectors these cross ratios have discontinuities which are simple functions of the cross ratios themselves. Patching together the different angular sectors one defines a Riemann Hilbert problem which consists in finding the corresponding analytic functions in each sector with the specified jumps between sectors. This problem can also be rewritten as an integral equation for the cross ratios as a function of ζ .

Intriguingly, this integral equation looks very much like a Thermodynamic Bethe Ansatz equation (TBA), or Y-system, for some particles whose physical significance is not clear to us. Moreover, the renormalized area can be expressed in terms of the cross ratios via a formula which is the same as the formula for the free energy of the Thermodynamic Bethe Ansatz.

This paper is organized as follows. In section two we recall some general properties of strings in AdS_5 . We review the Pohlmeyer reduction and the associated Hitchin system and flat connection. We explain how the linear problem for the flat connection lets us recover the surface. In section three we explain how to derive the TBA equation from the Hitchin system. First we use a WKB approximation to understand the behavior of the cross ratios as a function of ζ near $\zeta = 0, \infty$. With this information, we write down an integral equation. Finally we discuss some general aspects of the kinematics of the six-sided polygon.

The connection between classical differential equations and the TBA system for conformal quantum integrable theories was studied before in [14,15,16]. In fact, our results can be viewed as the extension of those results for massive integrable theories.

In section four we show that the area can be computed from the free energy of the TBA equations. We also discuss a family of exact solutions of the TBA system which corresponds to the large temperature limit, in the TBA language.

Finally, we present our conclusions.

2. Classical Strings in AdS_5

2.1. Pohlmeyer reduction and integrability

Classical strings in AdS spaces can be described by a reduced model which depends only on physical degrees of freedom [17,18,19,20,21,22,23]. We use embedding coordinates Y with $Y^2 = -1$. The conformal gauge equations of motion and the Virasoro constraints are

$$\partial\bar{\partial}Y - (\partial Y.\bar{\partial}Y)Y = 0, \quad \partial Y.\partial Y = \bar{\partial}Y.\bar{\partial}Y = 0 \quad (2.1)$$

where we parametrize the (spacelike) world-sheet in terms of complex variables z and \bar{z} . We can form an orthonormal basis $q = (q_0, \dots, q_5)$ with $q_0 = Y$, $q_4 = e^{-\alpha/2}\partial Y$, $q_5 = e^{-\alpha/2}\bar{\partial}Y$ and $q_I = B_I$ where I runs from 1 to 3.

$$e^\alpha \equiv \partial Y.\bar{\partial}Y, \quad B_I.Y = B_I.\partial Y = B_I.\bar{\partial}Y = 0, \quad B_I.B_J = h_{IJ} \quad (2.2)$$

The other inner products are fixed by the Virasoro constraints and the fact that $Y.Y = -1$. The real vectors B_I 's span the normal space to the world-sheet inside AdS_5 . We pick them to be orthonormal. The signature of the inner product h_{IJ} is $(-1, 1, 1)$ for standard Wilson loops in the usual $(3, 1)$ signature, $(-1, -1, 1)$ for Wilson loops in $(2, 2)$ signature

and $(-1, -1, -1)$ for Wilson loops in $(1, 3)$ signature¹. There is a residual gauge freedom, either $SO(1, 2)$, $SO(2, 1)$ or $SO(3)$ that rotate the B 's, which we don't fix, see [23] for gauge fixed equations.

B_3 can be set to a constant, reducing the problem to AdS_4 . Setting both B_3 and B_2 to a constant reduces the problem to AdS_3 . Given these vectors we can further define

$$v_I = B_I \cdot \partial^2 Y, \quad \bar{v}_I = B_I \cdot \bar{\partial}^2 Y \quad (2.3)$$

Note that with our conventions, as the B 's are real, v and \bar{v} are complex conjugate. We can define an $SO(2, 4)$ (or $SO(3, 3)$, or $SO(4, 2)$, depending on the signature of spacetime) flat connection on the worldsheet describing the parallel transport of q .

$$\partial q = -\mathcal{A}_z q, \quad \bar{\partial} q = -\mathcal{A}_{\bar{z}} q \quad (2.4)$$

Explicitly,

$$\mathcal{A}_z = - \begin{pmatrix} 0 & 0 & 0 & 0 & e^{\alpha/2} & 0 \\ 0 & 0 & d_1^2 & d_1^3 & 0 & -v_1 e^{-\alpha/2} \\ 0 & d_2^1 & 0 & d_2^3 & 0 & -v_2 e^{-\alpha/2} \\ 0 & d_3^1 & d_3^2 & 0 & 0 & -v_3 e^{-\alpha/2} \\ 0 & v^1 e^{-\alpha/2} & v^2 e^{-\alpha/2} & v^3 e^{-\alpha/2} & \partial\alpha/2 & 0 \\ e^{\alpha/2} & 0 & 0 & 0 & 0 & -\partial\alpha/2 \end{pmatrix} \quad (2.5)$$

Here $d_{IJ} = \partial B_I \cdot B_J$ and we lower and raise indices with h . $\mathcal{A}_{\bar{z}}$ is given by a similar expression obtained by interchanging $v \rightarrow \bar{v}$, $d_{IJ} \rightarrow \bar{d}_{IJ}$, permuting the last two rows and permuting the last two columns. The flatness condition for the connection \mathcal{A} is equivalent to the following equations [23]

$$\begin{aligned} \partial \bar{\partial} \alpha - e^\alpha - e^{-\alpha} v^I \bar{v}_I &= 0, \\ \partial \bar{v}_I - d_I^J \bar{v}_J &= 0, \quad \bar{\partial} v_I - \bar{d}_I^J v_J = 0, \\ e^{-\alpha} (\bar{v}_I v^J - v_I \bar{v}^J) &= f_I^J, \quad f \equiv \partial \bar{d} - \bar{\partial} d + [d, \bar{d}] \end{aligned} \quad (2.6)$$

f is the field strength of the gauge field d . These follow from the original equations (2.1). Conversely, one can first solve these equations, (2.6), and determine the connection \mathcal{A} . We

¹ These changes of signature correspond to the standard procedure of analytic continuation in the external momenta. In the field theory language, we are changing the external momenta but we are not changing the usual Feynman prescription for the internal momenta, in contrast to what was done in [24]. In particular, the IR divergencies have the same form in all signatures.

can then find six independent solutions of the linear problem (2.4). We can orthonormalize these solutions at some point. Then these six solutions will remain orthonormal throughout the worldsheet. We have now an orthogonal matrix q_I^A , where A labels the solution number and it is the spacetime index that all vectors q_I carry. The first row of the matrix, $q_0 = q_0^A = Y^A$, solves the original equations of motion and Virasoro constraints. The area is then given by

$$A = 2 \int d^2 z e^\alpha \quad (2.7)$$

This is the area in units where the radius of AdS is set to one². Then the amplitude or Wilson loop is given by [4]

$$\text{Amplitude} \sim \langle W \rangle \sim e^{-\frac{R^2}{2\pi\alpha'} A}; \quad \frac{R^2}{2\pi\alpha'} = \frac{\sqrt{\lambda}}{2\pi} \quad (2.8)$$

where we also have given the expression for the radius in terms of the 't Hooft coupling for $\mathcal{N} = 4$ SYM. For other theories we have other relations between the radius and the microscopic parameters, but our result will continue to be the leading approximation when $R^2/\alpha' \gg 1$.

An immediate consequence of (2.6) is that

$$\bar{\partial}(v^I v_I) = 0 \rightarrow v^I v_I = P(z) \quad (2.9)$$

with $P(z)$ some holomorphic function. Since q is a complete basis, we can write $\partial^2 Y$ in terms its elements

$$\partial^2 Y = \partial_\alpha \partial Y + v^I B_I \rightarrow P(z) = \partial^2 Y \cdot \partial^2 Y, \quad \bar{P}(\bar{z}) = \bar{\partial}^2 Y \cdot \bar{\partial}^2 Y \quad (2.10)$$

which gives a simple expression for this holomorphic function, and his anti-holomorphic companion, in terms of space-time quantities. Actually, one can verify directly from (2.1) that P defined as $P = \partial^2 Y \cdot \partial^2 Y$ is holomorphic. We can locally define a new variable w through

$$dw = P(z)^{1/4} dz \quad (2.11)$$

This can be viewed as a worldsheet conformal transformation $z \rightarrow w(z)$. In the new coordinates $\tilde{P}(w) = \left(\frac{\partial z}{\partial w}\right)^4 P(z) = 1$. This change of coordinates is locally well defined. However, at points where P has a zero, we have a branch cut in the w plane. We can view

² We have that $\int d^2 z = \int dx dy$, with $z = x + iy$.

the w plane as a sophisticated light-cone gauge choice. This w “plane” is useful to think about the asymptotic structure of the solution.

The integrability of the problem becomes manifest if we decompose \mathcal{A} in two parts, $\mathcal{A} = A + \Phi$, where A rotates (Y, B_I) and $(\partial Y, \bar{\partial} Y)$ separately among themselves, and Φ mixes them.

$$\begin{aligned}
A_z = - & \begin{pmatrix} 0 & 0 & 0 & 0 \\ 0 & 0 & d_1^2 & d_1^3 \\ 0 & d_2^1 & 0 & d_2^3 \\ 0 & d_3^1 & d_3^2 & 0 \\ & & & \partial\alpha/2 & 0 \\ & & & 0 & -\partial\alpha/2 \end{pmatrix} \\
\Phi_z = - & \begin{pmatrix} & & & & e^{\frac{\alpha}{2}} & 0 \\ & & & & 0 & -v_1 e^{-\frac{\alpha}{2}} \\ & & & & 0 & -v_2 e^{-\frac{\alpha}{2}} \\ & & & & 0 & -v_3 e^{-\frac{\alpha}{2}} \\ 0 & v^1 e^{-\frac{\alpha}{2}} & v^2 e^{-\frac{\alpha}{2}} & v^3 e^{-\frac{\alpha}{2}} & & \\ e^{\frac{\alpha}{2}} & 0 & 0 & 0 & & \end{pmatrix}
\end{aligned} \tag{2.12}$$

where the missing elements of the matrices are all zero. It is easy to show that $D = d + [A,]$ and Φ satisfy the Hitchin equations:

$$\begin{aligned}
D_z \Phi_{\bar{z}} = 0, \quad D_{\bar{z}} \Phi_z = 0, \\
[D_z, D_{\bar{z}}] + [\Phi_z, \Phi_{\bar{z}}] = 0
\end{aligned} \tag{2.13}$$

A simple consequence is that the spectral connection

$$\nabla_z^\zeta = D_z + \zeta^{-1} \Phi_z, \quad \nabla_{\bar{z}}^\zeta = D_{\bar{z}} + \zeta \Phi_{\bar{z}} \tag{2.14}$$

is flat for all values of the spectral parameter ζ . Notice that unless ζ is a phase, the connection lies in $SO(6, C)$.

One can solve the linear problem $\nabla^\zeta q[\zeta] = 0$ to define a whole family of solutions $q[\zeta]$. It is easy to verify that $Y[\zeta] = q_0[\zeta]$ is a complex solution of the usual equations of motion and Virasoro constraints. If ζ is a phase, $Y[\zeta]$ can taken to be real.

It turns out to be useful to study the action of the connection \mathcal{A} on spinors of $SO(2, 4)$ (or $SO(3, 3)$, or $SO(4, 2)$). In practice, we can pick a set of gamma matrices and use them to rewrite \mathcal{A} as a 4×4 matrix. With slight abuse of notation we will use the same symbol for the 6×6 and the 4×4 connections. We can keep the decomposition of \mathcal{A} into A and Φ simple, by using a set of gamma matrices adapted to their block-diagonal form:

$$\Phi_z = \begin{pmatrix} 0 & \frac{e^{-1/2\alpha}}{\sqrt{2}} v_I \tau^I \\ \frac{e^{1/2\alpha}}{\sqrt{2}} \mathbf{1}_2 & 0 \end{pmatrix} \quad A_z = \frac{1}{4} \begin{pmatrix} -\partial\alpha + d_{IJ} \tau^{IJ} & 0 \\ 0 & \partial\alpha + d_{IJ} \tau^{IJ} \end{pmatrix} \tag{2.15}$$

Here τ^I are appropriate Pauli matrices for $SO(1, 2)$, $SO(2, 1)$ or $SO(3)$. Furthermore, $\Phi_{\bar{z}} = \bar{\Phi}_z$ and $A_{\bar{z}} = -\bar{A}_z$, where the overline indicates hermitian conjugation, together with conjugation by either τ^1 or τ^{12} for the $SO(1, 2)$ or $SO(2, 1)$ cases.

Although Φ and A satisfy Hitchin's equations, they are not the most general solution. There is a simple constraint which can be added to Hitchin's equations, such that all solutions satisfying the constraint will be of the form (2.12). If we introduce the constant matrix

$$C = \begin{pmatrix} 0 & \sigma_2 \\ i\sigma_2 & 0 \end{pmatrix} \quad (2.16)$$

then the solutions of $CA^TC^{-1} = -A$ and $C\Phi^TC^{-1} = i\Phi$ have the form (2.15). Hence classical string solutions in AdS_5 correspond to solutions of Hitchin's equations which are fixed by the Z_4 automorphism $A \rightarrow -CA^TC^{-1}$ and $\Phi \rightarrow -iC\Phi^TC^{-1}$.

In terms of the vector-valued connections, we can construct a 6×6 matrix C combining a reflection of q_i , $i = 1, 2, 3$, and a rotation of $\pi/2$, $q_4 \rightarrow iq_4$, $q_5 \rightarrow -iq_5$, so that the Z_4 automorphism $A \rightarrow CAC^{-1}$ and $\Phi \rightarrow iC\Phi C^{-1}$ has fixed points of the form (2.12) only. In particular, the symmetry gives $\nabla^{i\zeta} = C\nabla^\zeta C^{-1}$, and $Y[\zeta]$ must be related to $Y[i\zeta]$ by a space-time rotation.

2.2. Boundary conditions for the connection at infinity

In this subsection we discuss the boundary conditions at infinity for the different components of the flat connection. We start with the simpler case of AdS_3 [25] and then express the boundary conditions in such a way that they are easy to generalize for the most general case.

The reduction to AdS_3 amounts to setting B_2 and B_3 to a constant. Hence $d_i^j = 0$, $v_2 = v_3 = 0$ and $v_1^2 = -P(z) \rightarrow v_1 = iP^{1/2}$. It turns out that in the AdS_3 case, P is the square of another polynomial $P \propto p^2$ [25]. Writing the four by four connections in terms of two by two blocks we obtain

$$A_z = \frac{1}{4}\partial\alpha \begin{pmatrix} -\mathbf{1}_2 & 0 \\ 0 & \mathbf{1}_2 \end{pmatrix}, \quad \Phi_z = \begin{pmatrix} 0 & \frac{e^{-\alpha/2}}{\sqrt{2}}P(z)^{1/2}\sigma_1 \\ \frac{e^{\alpha/2}}{\sqrt{2}}\mathbf{1}_2 & 0 \end{pmatrix}, \quad A_{\bar{z}} = -A_z^\dagger, \quad \Phi_{\bar{z}} = \Phi_z^\dagger \quad (2.17)$$

Flatness condition implies the following equation for α

$$\partial\bar{\partial}\alpha - e^\alpha + e^{-\alpha}|P(z)| = 0 \quad (2.18)$$

This generalized sinh-Gordon equation can be brought to a more standard form by defining a new variable w such that $dw = P(z)^{1/4}dz$, (2.11), and making a field redefinition

$$\alpha = \hat{\alpha} + \frac{1}{4} \log P(z) \bar{P}(\bar{z}) \quad (2.19)$$

As argued in [26,25], the appropriate boundary conditions are that $\hat{\alpha}$ vanishes at infinity, decaying exponentially. One simple way to understand this is to notice that the four cusp solution is simply $\hat{\alpha} = 0$ and $P = 1$. After we go to the w plane, this is indeed the asymptotic behavior at large w for any polynomial P . This is what we expect, since near each cusp the solution should be very similar to the four cusp solution. In the four cusp solution the w plane and the z plane coincide and we have four cusps corresponding to the four quadrants of the w plane. For a polynomial of degree N which goes as $P \sim z^N + \dots$ we have that $w \sim z^{\frac{N+4}{4}}$. This implies that going once around the z plane we go around the w plane $\frac{N+4}{4}$ times. This implies that the total number of quadrants in the w plane is $n = N + 4$. This is the total number of cusps. In conclusion, a polynomial of degree N leads to an $n = N + 4$ sided polygon.

Such boundary conditions can be understood in the following alternative way. If we set $\hat{\alpha} = 0$, then we can diagonalize Φ and A by an honest gauge transformation h (the exponential of an anti-hermitian matrix)

$$h^{-1}\Phi_z h = \frac{1}{\sqrt{2}} \begin{pmatrix} P(z)^{1/4} & & & \\ & -iP(z)^{1/4} & & \\ & & -P(z)^{1/4} & \\ & & & iP(z)^{1/4} \end{pmatrix} \equiv \Phi_z^{diag} \quad (2.20)$$

$$h^{-1}A_z h + h^{-1}\partial h = 0$$

The statement that $\hat{\alpha} \rightarrow 0$ at infinity is equivalent to saying that exists a gauge transformation such that

$$h^{-1}\Phi_z h \rightarrow \Phi_{diag}, \quad h^{-1}A_z h + h^{-1}\partial h \rightarrow 0$$

at infinity. We have similar expressions for $\Phi_{\bar{z}}$, $A_{\bar{z}}$ with the same h .

The boundary conditions at infinity for the general case of AdS_5 can be stated in a similar way. After all, near each cusp we expect the same behavior as the one for the four cusp solution. In fact, these are standard boundary conditions from the point of view of the Hitchin system. There exist a gauge transformation such that $h^{-1}\Phi_z h \rightarrow \Phi_{diag}$ and $h^{-1}\Phi_{\bar{z}} h \rightarrow \Phi_{diag}^*$ at infinity. Notice that the boundary conditions $h^{-1}\Phi_{\bar{z}} h \rightarrow \Phi_{diag}^*$ involve

a simple complex conjugation. We also have that $\hat{\alpha} \rightarrow 0$ at infinity, where $\hat{\alpha}$ is given by (2.19).

For the case of AdS_3 and AdS_4 the matrix $d_{IJ}\tau^{IJ}$ is diagonal, and has an off-diagonal component only for the case of AdS_5 . Next, we consider A_z in the same basis that diagonalizes $\Phi_{\bar{z}}$ at infinity. Flatness of $\Phi_{\bar{z}}$ requires A_z to be diagonal as well. There are two further requirements: in the original basis A_z should be block-diagonal, and single-valued. This imposes the following boundary conditions

$$h^{-1}A_z h + h^{-1}\partial h \rightarrow \frac{m}{z} \begin{pmatrix} \sigma_3 & 0 \\ 0 & \sigma_3 \end{pmatrix}, \quad h^{-1}A_{\bar{z}} h + h^{-1}\bar{\partial} h \rightarrow \frac{\bar{m}}{\bar{z}} \begin{pmatrix} \sigma_3 & 0 \\ 0 & \sigma_3 \end{pmatrix} \quad (2.21)$$

where \bar{m} is minus the conjugate of m for (3,1) or (1,3) signature and plus the conjugate of m for (2,2) signature. The constant m is allowed to be non-zero only for a $P(z)$ of even degree n : in the diagonal basis, Φ_{diag} comes back to itself under $z \rightarrow e^{2\pi i} z$ up to conjugation by a shift matrix. In that basis, our asymptotic choice for A is invariant under that shift only for even n . Note that the Z_4 action that restricts the form of the general Hitchin equation to our form (discussed around (2.16)) has a simple action in the basis that diagonalizes Φ (2.20). The matrix C simply performs a cyclic permutation of all four eigenvalues. It also permutes the eigenvalues of A . Thus the condition $A = -CA^T C^{-1}$ implies that A has the matrix structure in (2.21).

As already mentioned, for the cases of AdS_3 and AdS_4 , the gauge field is diagonal before the gauge transformation. In particular, its structure forbids the extra term in (2.21). This term is present only for the case of AdS_5 . This is related to the fact that, for $AdS_{3,4}$, once we choose a polynomial $P(z)$, there is a unique solution satisfying the appropriate boundary conditions, but this is not the case for AdS_5 .

We can use these observations also to count the number of parameters that we expect in general. In order to count the moduli of the Hitchin equations we can go to the region where the zeros of the polynomial are widely spaced. In this region the matrix Φ is diagonal in most of the space. Let us start by counting the number of parameters in the polynomial P . We can always set the coefficient of the highest power to one by a rescaling of z . We can also set the coefficient of the next term to zero by a translation. Thus we have only $N - 1$ complex coefficients left. As we explained above, as long as we can set $\hat{\alpha} \sim 0$ we can also diagonalize A . We will then have various Wilson lines for the connection around various one cycles of the surface. In order to have a non-zero value for the Wilson line we need a one cycle that is consistent with the Z_4 projection. Instead of counting one

cycles we can count differential forms which are odd under the generator of Z_4 . We have a curve $x^4 = P(z)$ with the differential xdz . The Z_4 projection on the Hitchin system maps $x \rightarrow ix$. The one forms can be written as $\eta = q(z)\frac{dz}{x^2}$. For large z we require that they decay as $\frac{1}{z^2}dz$ or faster. The one form decaying as $1/z$ was already included in the discussion around (2.21). For a polynomial of even degree N we have $q \sim z^{N/2-2} + \dots$. We have $N/2 - 1$ complex coefficients³. The total number of real parameters is then $2(N - 1) + 1 + 2(N/2 - 1) = 3(N - 1) = 3n - 15$ which is the expected number of independent cross ratios for an n sided polygon (recall that $n = N + 4$).

2.3. Behavior at infinity of the solutions of the linear problem

Here we show that the above conditions on the connection imply that the solutions of the linear problem are such that the surface ends on the boundary of AdS on a polygonal contour with light-like sides.

The above boundary conditions imply that the behavior at infinity of the flat section q is controlled by the degree N of the polynomial P . The large $|z|$ region is divided into $n = N + 4$ angular sectors of equal width. In the sector V_i the six components of Y grow exponentially with a specific fixed ratio, so that the worldsheet reaches a specific point x_i at the boundary, where the i -th cusp resides. Alternatively, $Y \sim y_i \exp S(z)$ where $S(z)$ grows like a power of $|z|$ and y_i is a null vector, which identifies a point on the boundary of AdS_5 .

Here we can think of the boundary of AdS_5 as the set of null vectors $y \in R^{2,4}$ with $y^2 = 0$, together with the identification $y \sim \lambda y$. Thus, only the direction of the null vector y is important⁴.

As we change sectors, the point x_i (or y_i) on the boundary jumps, in a way which is well described by Stokes theory for the flat connection \mathcal{A} . It is useful to consider the spinor version of the connection. Let ψ_a be a set of four linearly independent spinor flat sections satisfying

$$\partial\psi_a = -\mathcal{A}_z\psi_a, \quad \bar{\partial}\psi_a = -\mathcal{A}_{\bar{z}}\psi_a \quad (2.22)$$

³ The fact that the dz/z term counts as only one real coefficient is related to the fact that we just have one compact cycle associated to this one form, which is a circle around infinity.

⁴ More explicitly, we can say $y = (y_+, y_-, y_\mu)$, $\mu = 0, 1, 2, 3$. $y^2 = y_+y_- + y_\mu y_\mu = 0$. Then $x_\mu \equiv \frac{y_\mu}{y_+}$ are the ordinary Poincare coordinates. Also, given two points y and \tilde{y} we have that $2y \cdot \tilde{y} = -y_+ \tilde{y}_+ (x - \tilde{x})^2$. Thus, the inner product of two y vectors is proportional to the distance in $R^{1,3}$. If we form cross ratios the proportionality factors cancel. Thus cross ratios can be written in terms of ratios of products of projective y vectors.

We can write a general solution to the vector-valued linear problem as

$$q_I^A \gamma_{A ab} = \psi_{\alpha a} \Gamma_I^{\alpha\beta} \psi_{\beta b} \quad (2.23)$$

Here γ_{ab}^A are the six space-time gamma matrices. a, b are space-time spinor indices. Γ_I are the six gamma matrices used to convert the connection \mathcal{A} from the vector to the spinor representation. α, β are internal spinor indices. These are the indices acted upon by the connection. Both gamma matrices are antisymmetric in their indices.

The boundary conditions described above imply the existence of n sectors W_i (displaced by $\frac{\pi}{n}$ with respect to the V_i) in which the ψ^a grow exponentially at large $|z|$. Much like in the vector case, this determines a direction (a “twistor”) $\lambda_{a,i}$ in each sector, as $\psi_{\alpha a} \sim \lambda_{a,i} e_{\alpha,i} \exp \tilde{S}(z)$, where e_{α} is the direction of this growing solution in the internal space. The location of the space-time cusp associated to a sector V_i is determined by the twistors for the sectors W_i and W_{i+1} overlapping with V_i .

$$y_i^A \gamma_{A ab} = (\lambda_{a,i} \lambda_{b,i+1} - \lambda_{b,i} \lambda_{a,i+1}) (e_{\alpha,i} \Gamma_0^{\alpha\beta} e_{\beta,i+1}) \quad (2.24)$$

Γ_0 appears here because the component $q_0 = q_0^A$ is the solution Y^A . The spinors $\lambda_{a,i}$ are determining the direction of the vector y_i^A . The factor in parenthesis is simply an overall scale. Thus, we can assign a spinor λ_i to each side of the polygon. The vertices of the polygon are then given by $y_i \sim \lambda_i \lambda_{i+1}$. These spinors are the same as the momentum twistors introduced in [27].

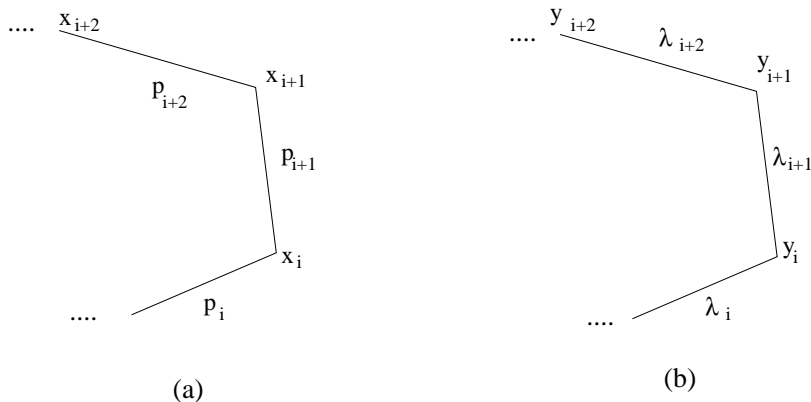


Fig. 2: In (a) we see the polygon labeled by the position of the vertices x_i , or equivalently, the momenta p_i . In (b) we see how the data defining the polygon emerges in our case. We have a spinor of $SU(2|2)$ ψ associated to each edge. The positions of the vertices y_i are bilinears of spinors. These coincide with the momentum twistors introduced in [27].

The inner product can be written as ⁵

$$y \cdot y' = (y \cdot \gamma_{ab})(y' \cdot \gamma_{cd})\epsilon^{abcd} = \det(\lambda_1 \lambda_2 \lambda'_1 \lambda'_2) \quad (2.25)$$

where $\lambda_{1,2}$ are the two spinors producing y and $\lambda'_{1,2}$ are the two spinors producing y' . It is then clear that not only $y_i^2 = 0$, but also $y_i \cdot y_{i+1} = 0 = (x_i - x_{i+1})^2$, hence the sides of the boundary polygon are null, as desired.

2.4. Linear problem at infinity and Stokes phenomena

In this subsection we describe the nature of the Stokes phenomenon at large z . We also express the Stokes data in terms of the spacetime cross ratios.

Once we have understood the asymptotic form of the connection, it is straightforward to understand the asymptotic form of the solutions ψ_a of the linear problem (2.22). As already mentioned, we can perform a gauge transformation in such a way that both Φ_z and $\Phi_{\bar{z}}$ become diagonal at infinity. In such basis, a generic solution takes the asymptotic form

$$\psi \approx e_1 z^m \bar{z}^{\bar{m}} e^{\frac{1}{\sqrt{2}}(w+\bar{w})} + e_2 z^{-m} \bar{z}^{-\bar{m}} e^{-\frac{i}{\sqrt{2}}(w-\bar{w})} + e_3 z^m \bar{z}^{\bar{m}} e^{-\frac{1}{\sqrt{2}}(w+\bar{w})} + e_4 z^{-m} \bar{z}^{-\bar{m}} e^{\frac{i}{\sqrt{2}}(w-\bar{w})} \quad (2.26)$$

where $w = \int P(z)^{1/4} dz \sim z^{\frac{n}{4}}$, $\bar{w} = \int \bar{P}(\bar{z})^{1/4} d\bar{z} \sim \bar{z}^{\frac{n}{4}}$. This asymptotic solution is a rather reliable approximation of the exact solution at large $|z|$, as long as one restricts the range of $\arg z$ appropriately. The failure of the approximation is governed by Stokes phenomena. Consider the behavior of a generic approximate solution as one varies $\arg z$ at large $|z|$: the four exponential terms will take turns at controlling the asymptotic behavior, so that ψ will be proportional to, say, e_1 whenever $Re w$ is positive and bigger than $|Im w|$ so that $(w + \bar{w})$ is the largest exponent. A generic exact solution will have a similar behavior, and in each sector

$$W_i : \frac{2\pi}{n}i - \frac{3\pi}{n} < \arg z < \frac{2\pi}{n}i - \frac{\pi}{n}$$

it will point in some direction λ_i , but λ_{i+4} does not have to coincide with λ_i . We will denote as S_i the appropriate largest exponent.

⁵ The determinant of $(\lambda_1, \lambda_2, \lambda_3, \lambda_4)$ is equal to $\epsilon^{\alpha\beta\gamma\delta} \lambda_{\alpha,1} \lambda_{\beta,2} \lambda_{\gamma,3} \lambda_{\delta,4}$.

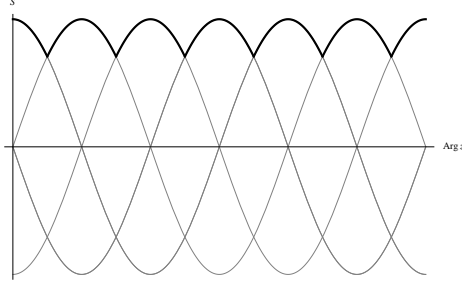


Fig. 3: The light lines show the four exponents of the WKB approximation for large $|z|$ as a function of the argument of z . The darker line follows the behavior of a typical solution. A typical solution is the superposition of all four solutions so that the largest exponent dominates.

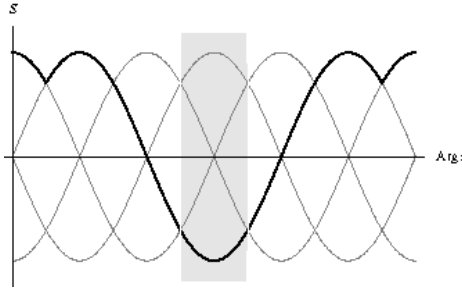


Fig. 4: The dark line shows the behavior of a "small solution" as we change the argument of z . The solution is controlled by the smallest exponent in the darkened angular sector. The solution is still controlled by the same exponent as we move away from the darkened region, until the exponent grows to a maximum. Subsequently, it behaves as the generic solution, see fig. 3.

There is a simple, powerful fact: if we pick a ray towards $|z| \rightarrow \infty$ away from the boundaries of the W_i , we can identify a unique (up to rescaling) exact solution by the boundary condition which requires the fastest possible decay at infinity. This small solution s_i is the same for all rays inside W_i . More generally, one can identify uniquely k -dimensional subspaces of solutions whose growth is controlled by the k smallest exponentials. That way, it is easy to see that s_i will still behave as $\exp S_i$ if continued beyond W_i , through W_{i-1} and W_{i-2} or through W_{i+1} and W_{i+2} , as S_i grows all the way to be the largest exponent see fig. 4 . Beyond that, the behavior of s_i is unconstrained.

One can generically take the set $(s_i, s_{i+1}, s_{i+2}, s_{i+3})$ to be a neat basis of linearly independent solutions. This implies that s_{i+4} can be expressed in terms of a linear combination of the previous four solutions. In the sector where s_{i+2} is the smallest solution, s_i and s_{i+4} are the two largest solutions. Thus we can compare them. We choose to normalize s_{i+4} so

that it is proportional to $-s_i$ in this sector, up to corrections by smaller solutions. Thus we can write

$$s_{i+4} + s_i = a_{i+1}s_{i+1} + b_{i+2}s_{i+2} + c_{i+3}s_{i+3}.$$

With this choice of normalization we have that $\det(s_i, s_{i+1}, s_{i+2}, s_{i+3}) = 1$. We should impose the periodicity constraint $s_{i+n} = \mu_i s_i$. We can relate the μ_i with the formal monodromies, i.e. the monodromies of the approximate asymptotic solutions. The formal monodromy receives contributions from both m, \bar{m} and the coefficient in front of $1/z$ in the expansion of $P(z)^{1/4}$, if present. The simplest example is the pentagon. There are no formal monodromies, and $s_1 + s_2 + s_3 + s_4 + s_5 = 0$ is the unique way to solve all the constraints.

The example of interest for us is the hexagon. In this case our relation requires $s_1, s_5, s_9, s_{13} = \mu_1^2 s_1$ to grow with the same exponent $S_1(z)$, but the comparison is made after going around the z plane twice, hence $\mu_1^2 = \exp(S_1(e^{4\pi i}z) - S_1(z))$, and μ_1 agrees up to a sign with the formal monodromy. The formal monodromies come from m, \bar{m} (2.21) only. We can set without loss of generality $P(z) = z^2 - U$, and then $P(z)^{1/4} = z^{1/2} - \frac{U}{4z^{3/2}} + \dots$ has an expansion in half integer powers of z^{-1} and there is no logarithm⁶ in w . Hence we get formal monodromies $s_7 = \mu s_1, s_8 = \mu^{-1} s_2, s_9 = \mu s_3, s_{10} = \mu^{-1} s_4$, etc. Here $\mu = \pm \exp 2\pi i(m - \bar{m})$. In $(3, 1)$ signature, μ is a phase, while in $(2, 2)$ signature μ is a real number.

The coefficients b_i will play a particularly important role in what follows, since for $n = 6$ they contain the non-trivial Stokes information. Consider the determinant $\det(s_i, s_{i+1}, s_{i+3}, s_{i+4}) = -b_{i+2}$. For the hexagon that is the same as

$$b_{i+2} = -\mu\mu^{-1} \det(s_{i+6}, s_{i+7}, s_{i+3}, s_{i+4}) = b_{i+5}$$

It turns out that everything can be expressed in terms of μ, b_1, b_2, b_3 , subject to the relation^{7,8}

$$b_1 b_2 b_3 = b_1 + b_2 + b_3 + \mu + \mu^{-1} \qquad b_{i+3} = b_i \qquad (2.27)$$

⁶ More explicitly, in cases where N is a multiple of four, we will get that generically we have $dw = (z^{N/4} + \dots + \tilde{m}/z + \dots)dz$ which implies that w contains a term going like $w \sim \dots + \tilde{m} \log z + \dots$. Such a term also contributes to the formal monodromy.

⁷ We can change $b_i \rightarrow -b_i$ and $\mu \rightarrow -\mu$ by changing the signs of some of the s_i . Thus these two possibilities describe the same physical situation. In this paper we concentrate in the regime where the sign of all b_i s are the same, which we take to be positive. Then the two signs of μ describe two different physical situations.

⁸ The $\mu = 1$ limit of this equation was obtained in the study of the x^4 anharmonic oscillator in [14].

The case of the hexagon in AdS_3 is particularly important. Then, the solutions at even and odd sectors do not mix, and satisfy $s_1 - s_3 + s_5 = 0$ and $s_2 - s_4 + s_6 = 0$, so that $b_i = 1$ identically, and $\mu = -1$, as it should. For the AdS_4 case we have that $\mu = \pm 1$.

To conclude this subsection, we would like to relate the b_i to the space-time cross-ratios for the case of the hexagon. If we are given a solution q_I of the vector problem, there is a very simple way to extract the position of the cusps. The bilinear $s_i^T \Gamma^I s_{i+1}$ gives the vector solution which decays the fastest in the sector V_i , hence the contraction $y_i^A = q_I^A s_i^T \Gamma^I s_{i+1}$ gives the position of the cusp. The inner product is

$$y_i \cdot y_j = (q_I \cdot q_J) s_i^T \Gamma^I s_{i+1} s_j^T \Gamma^J s_{j+1} = s_i^T \Gamma^I s_{i+1} s_j^T \Gamma^J s_{j+1} = \det(s_i, s_{i+1}, s_j, s_{j+1}).$$

Hence the cross-ratios are

$$u_1 = \frac{x_{13}^2 x_{46}^2}{x_{14}^2 x_{36}^2} = \frac{1}{b_2 b_3}, \quad u_2 = \frac{x_{24}^2 x_{15}^2}{x_{25}^2 x_{14}^2} = \frac{1}{b_1 b_3}, \quad u_3 = \frac{x_{35}^2 x_{26}^2}{x_{36}^2 x_{25}^2} = \frac{1}{b_1 b_2} \quad (2.28)$$

In conclusion, we have shown that the Stokes data at infinity is given by b_1, b_2, b_3 and μ with the constraint (2.27). The spacetimes cross ratios are related to the b_i via (2.28).

3. From Hitchin to TBA

If we introduce now the spectral parameter, ζ , in the connection, we can investigate the behavior of the deformed solution $Y[\zeta]$. As the conserved polynomial becomes simply $\zeta^{-4} P(z)$, the deformed solution will have the same number of cusps at infinity, associated with directions $y_j[\zeta]$ and cross-ratios $u_j[\zeta]$ (or $b_j[\zeta]$) which are meromorphic in ζ away from $\zeta = 0, \infty$. The only slight subtlety is that the location of the sectors $W_j[\zeta]$ and $V_j[\zeta]$ varies as the phase of ζ varies. The sectors $W_j[\zeta]$ are defined by

$$W_j[\zeta] : \frac{2\pi j}{n} + \frac{4}{n} \arg \zeta - \frac{3\pi}{n} < \arg z < \frac{2\pi j}{n} + \frac{4}{n} \arg \zeta - \frac{\pi}{n}.$$

Hence the small sections $s_j[\zeta]$, the coefficients $b_j[\zeta]$ and the cross-ratios $u_j[\zeta]$ do not quite come back to themselves as $\zeta \rightarrow e^{2\pi i} \zeta$, but rather undergo a shift in the index $j \rightarrow j + 4$, $b_j[\zeta e^{2\pi i}] = b_{j+4}[\zeta]$. Due to the Z_4 automorphism of A, Φ , there is actually a symmetry $b_j[i\zeta] = b_{j+1}[\zeta]$. We will not make use of this symmetry for now. Note that, for the hexagon case, the relation (2.27) that we had for $\zeta = 1$ remains valid for $b_i[\zeta]$, with μ independent of ζ . Throughout this section we will hold U and μ fixed and we will only vary ζ . Of course, we are only interested in the values at $\zeta = 1$. We will determine these values by writing an equation for the cross ratios as a function of ζ and then we will set $\zeta = 1$. This equation comes from demanding that the functions are analytic plus the statement that they have a known approximate expression (displaying Stokes phenomenon) near $\zeta \sim 0, \infty$, which can be computed via the WKB approximation.

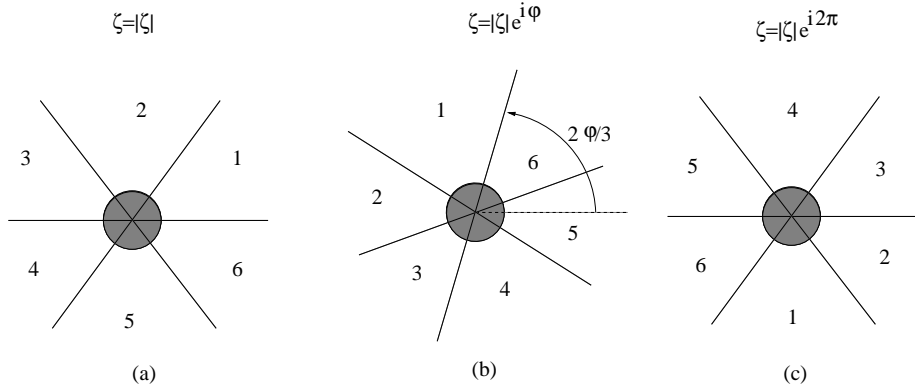


Fig. 5: This figure shows the sectors in the z plane for the case of $n = 6$. They could be the sectors W_j or V_j . In (a) we see the various sectors for a given value of the phase of ζ . (b) as we change the phase of ζ by $\zeta \rightarrow \zeta e^{i\varphi}$ the sectors rotate by an angle $2\varphi/3$. In (c) we see the result of a full rotation $\zeta \rightarrow \zeta e^{i2\pi}$. We come back to (a) up to a relabeling of sectors.

We aim to set up a Riemann-Hilbert problem, and derive a useful set of integral equations from it. The equations take the appearance of TBA equations. Although the resemblance is purely formal, it is rather striking. The TBA equations do not just compute the cross-ratios. We will show how the regularized area of the minimal surface, which can be written as a suitably regularized integral of $Tr\Phi\bar{\Phi}$, takes the form of the free energy for the TBA equations.

For the sake of simplicity, we will give a direct derivation of the TBA equations for the case at hand. The reader should be aware that this is a special case of a much broader result. The monodromy data (such as the cross-ratios) of the auxiliary connection for any Hitchin system is always computed by a TBA-like set of equations. Physically, this fact follows from a relation between Hitchin systems and $\mathcal{N} = 2$ gauge theories [28,29]. In the special case of $SU(2)$ Hitchin systems, the result has been demonstrated directly, and a crucial ingredient for the TBA equations (the spectrum) has been determined through a simple WKB analysis [29]. For more general higher rank systems, the simple WKB analysis is expected to fail, and be replaced by something more complicated, and currently unknown. Luckily for us, the special Hitchin systems with a simple spectral curve $x^m = P(z)$, such as the one relevant for the minimal surfaces in AdS_5 , are still amenable to a simple WKB analysis, although an extra layer of analysis is required. The relation between the regularized integral of $Tr\Phi\bar{\Phi}$ and the TBA free energy appears to be valid for general Hitchin systems as well, and was not noticed in previous works.

3.1. WKB approximation of $b_i[\zeta]$

Near $\zeta = 0, \infty$ the behavior of the connection is clearly dominated by Φ and $\bar{\Phi}$ respectively, and we can use a WKB approximation to evaluate the behavior of the cross-ratios. The basic idea behind the WKB approximation is to go to a (complex) gauge where, say, both Φ and \bar{A} have been diagonalized. If one ignores the higher order corrections as $\zeta \rightarrow 0$, the i -th component of a flat section should behave like $\exp \frac{1}{\zeta} \int x_a dz$, where x_a are the eigenvalues of Φ . The higher order corrections mix the different components of the flat section, and disrupt this simple exponential behavior. The component with the highest exponential growth (largest real part of $\frac{xdz}{\zeta}$) will in general contaminate all the others, but its leading exponential growth will be unaffected. The simple WKB approximation computes the small ζ exponential behavior of a flat section transported along a path for which the real part of $\frac{xdz}{\zeta}$ for a given eigenvalue remains the largest. This is called a ‘‘WKB path’’: the condition guarantees that the flat section grows with the largest exponent and is well described by the WKB approximation.

In the case at hand, we want to compare the ‘‘small’’ flat vector-valued sections $s_i^T \Gamma^I s_{i+1}$ at the rays r_i between the sectors W_i and W_{i+1} . At sufficiently large z , the small section is, by definition, the flat section which grows the fastest along a line which goes towards smaller z along that ray r_i . If we can find a WKB path which flows all the way to some other ray r_j at large z , we can evaluate the small ζ asymptotics of the inner product $\det(s_i, s_{i+1}, s_j, s_{j+1})$ as $\exp \frac{1}{\zeta} \int_{p_i}^{p_j} x dz$. $p_{i,j}$ are some reference points near $z = \infty$ in $r_{i,j}$. Varying p_i, p_j changes the (arbitrary) choice of normalization for the small sections. Remember that the eigenvalue x for the vector-valued connection will be the sum of two consecutive roots $P(z)^{1/4}$. If we have appropriate WKB paths available for all the pieces of a cross-ratio, and we can evaluate the asymptotic behavior of each piece and combine them. The spurious dependence on the p_i drops off from the cross-ratio, and the various contour integrals join into a single integral of $P(z)^{1/4}$ along an appropriate contour on the Riemann surface $x^4 = P(z)$.

The eigenvalues x_a for the vector valued Φ are of the general form $x, -ix, -x, ix, 0, 0$. The real part of $\zeta^{-1} x dz$ is the largest if the phase of $\zeta^{-1} x dz$ sits inside an open sector of width $\pi/2$ centered around the positive real axis. Beyond that sector, either $\zeta^{-1}(-ix) dz$ or $\zeta^{-1}(ix) dz$ will have a larger real part. This is the condition which must be satisfied by a WKB path. It is particularly useful to consider WKB paths of steepest ascent, such that the phase φ of $x dz$ is constant. Such a path satisfies the WKB condition

for all values of ζ inside a sector of width $\pi/2$ centered around the ray of phase φ in the ζ plane. Correspondingly, any estimate of a cross-ratio asymptotics done with WKB paths of constant phase φ will hold along all rays inside the corresponding sector in the ζ plane. Notice that the WKB condition is satisfied in the sector both with respect to $\zeta^{-1}xdz$ and to $\zeta\bar{x}\bar{d}z$, so the same calculation controls the asymptotics both at small and at large $|\zeta|$ for a given phase of ζ .

The WKB paths of constant phase φ are straight lines in the w plane. At sufficiently large z , away from the zeros of $P(z)$, there are always WKB paths joining rays r_i and r_{i+2} , which give estimate of the reference inner products $(s_i \wedge s_{i+1} \wedge s_{i+2} \wedge s_{i+3})$. The straight lines in the w plane can be grouped in continuous families which asymptote to the same rays at infinity. Different families are separated by the special lines which end on the zeros of $P(z)$. It is useful to draw a picture in the z plane, with one WKB path from each family for a given choice of φ (and all possible choices of a fourth root of $P(z)$).

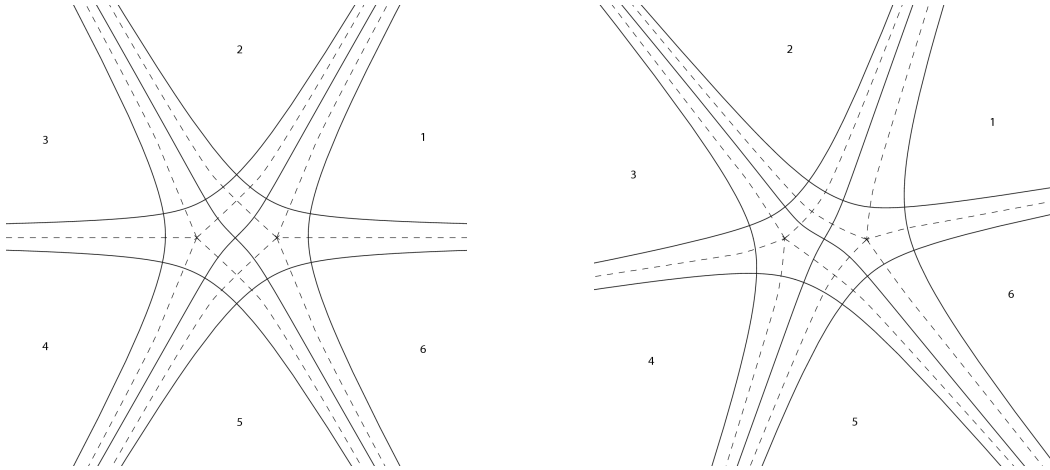


Fig. 6: This figures shows WKB lines in the z plane with a constant phase. The dotted lines end at the zeros and they divide various regions. WKB lines that cross at 90 degrees correspond to two different eigenvalues that differ by an i factor. Solid lines show lines that we will use to evaluate b_3 and b_1 in this case. The figure on the right shows the effect of increasing the value of φ . Note that we have WKB lines joining cusps 12 with 45 and 23 with 56 but we do not have WKB line joining 16 with 34.

We see that only two out of three opposite pairs of rays are joined by a WKB path, which allows the estimate of $(s_i \wedge s_{i+1} \wedge s_{i+3} \wedge s_{i+4})$. See fig. 6. As one varies the value of φ continuously, the configuration of paths of constant phase also varies continuously. Jumps happen at special values of φ , where the special WKB paths ending on a zero of

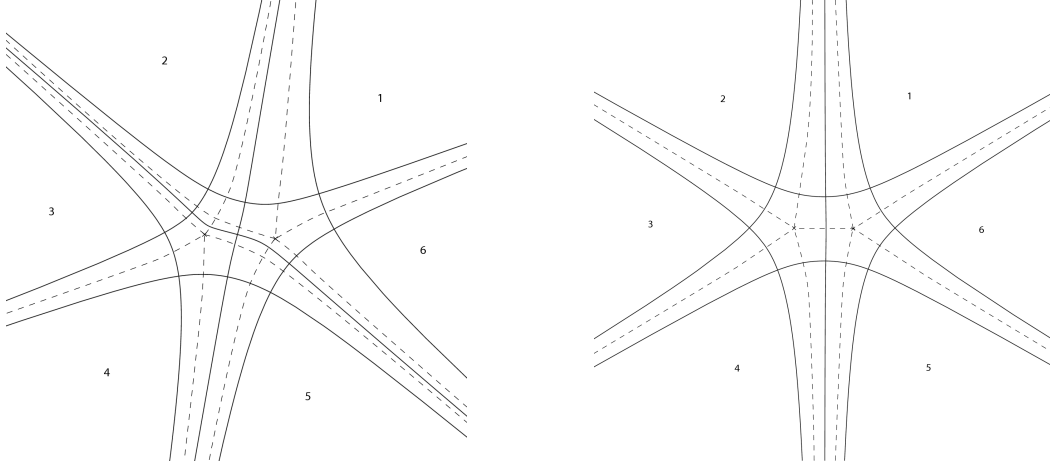


Fig. 7: These are the same WKB lines as in the previous figure but for increasing values of φ . The figure on the right represents a critical value of the phase where the line that was joining the cusp 23 with 61 no longer exists. Instead we have WKB lines that end at zeros and a new WKB line that joins the two zeros. In this case we can only use the WKB approximation to compute the cross ratio b_1 involving cusps 12 with 45.

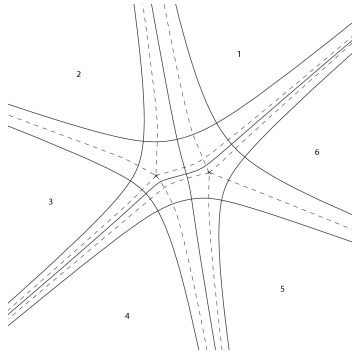


Fig. 8: This figure shows the WKB lines for a phase which is bigger than the critical phase. In this case we have WKB lines joining the cusps 12 with 45 and also joining 16 with 34. In this case we can compute b_2 and b_3 via the WKB approximation.

$P(z)$ collide with the other zero, see fig. 7. Clearly, the special values of φ coincide with the phase of the integral of $x dz$ from a zero to the other along that path. Since x is the sum of two eigenvalues of the spinor connection, we have $x = \frac{(1+i)}{\sqrt{2}}(z^2 - U)^{1/4}$, see (2.20). We can rescale $z \rightarrow U^{1/2}t$ to get $x dz = U^{3/4}(1-t^2)^{1/4}dt$. The path runs on real t between $t = -1$ and $t = 1$, the special values φ_i are the phases of the four roots of $U^{3/4}$. At each φ_i a single pair of opposite rays (which we can identify without loss of generality with r_i and r_{i+3}) are joined by a WKB path of constant phase. The path exists in the whole range

$\varphi_{i+1} < \varphi < \varphi_{i-1}$, i.e. $\varphi_i - \pi/2 < \varphi < \varphi_i + \pi/2$. Hence the product $(s_i \wedge s_{i+1} \wedge s_{i+3} \wedge s_{i+4})$ has a simple WKB estimate for a range of

$$\varphi_i - 3\pi/4 < \arg \zeta < \varphi_i + 3\pi/4.$$

We can use this information to estimate the behavior of $b_i[\zeta]$ as $\zeta \rightarrow 0$ and $\zeta \rightarrow \infty$ inside this sector. We find $\exp Z_i/\zeta$ at small $|\zeta|$ and $\exp \bar{Z}_i \zeta$ at large $|\zeta|$ on the whole sector $\varphi_i - 3\pi/4 < \arg \zeta < \varphi_i + 3\pi/4$ for an appropriate function $Z_i[U]$. Patiently assembling the WKB phase integrals for all the pieces of the cross-ratio, Z_i is

$$Z = U^{3/4} \int_{-1}^1 dt (1-t^2)^{1/4} dt = \frac{\sqrt{\pi} \Gamma(\frac{1}{4})}{3\Gamma(\frac{3}{4})} U^{3/4} \quad (3.1)$$

The different Z_j corresponds to the four roots of $U^{3/4}$. The specific root of $U^{3/4}$ is exactly the one with phase φ_j , hence b_j is exponentially large in the half plane $\varphi_j - \pi/2 < \varphi < \varphi_j + \pi/2$. The asymptotic behavior of b_j changes beyond the lines at $\varphi_j \pm 3\pi/4$. We can check this explicitly using the relation (2.27). For example, we can write

$$b_j = (\mu + \mu^{-1} + b_{j-1} + b_{j-2}) / (b_{j-1} b_{j-2} - 1).$$

As we cross the ray at $\varphi_j + 3\pi/4$, b_{j-1} and b_{j-2} switch dominance, and the asymptotic value of the ratio passes from $b_j \sim b_{j-2}^{-1} \sim \exp[Z_j/\zeta]$ to $b_j \sim b_{j-1}^{-1} \sim \exp[-Z_{j-1}/\zeta] \sim \exp[-iZ_j/\zeta]$. On the other side, beyond the ray at $\varphi_j - 3\pi/4$ we get $b_j \sim b_{j+1}^{-1} \sim \exp[-Z_{j+1}/\zeta] \sim \exp[iZ_j/\zeta]$.

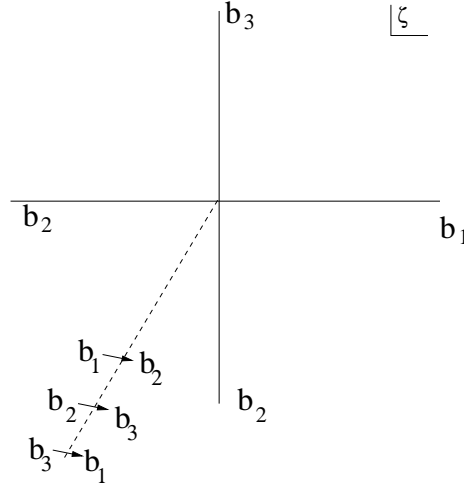


Fig. 9: We are displaying the ζ plane for a particular value of the phase of U , chosen so that along the positive real axis, $b_1[\zeta]$ becomes largest. Along the positive imaginary axis, $b_3[\zeta]$ is the largest, and so on. Due to the fact that the $b_j[\zeta e^{2\pi i}] = b_{j+4}[\zeta] = b_{j+1}[\zeta]$ we have a branch cut, denoted by the dotted line where we switch the indexing of the b_j . We have indicated what each b_j changes into. As we change the phase of U the lines where b_i are the biggest rotate rigidly.

This is all the information we will need from the WKB analysis.

3.2. A Riemann-Hilbert problem

In this subsection we set up a Riemann-Hilbert problem. For this we need to combine the fact that the $b_j[\zeta]$ are meromorphic in ζ (except for $\zeta = 0, \infty$) with the fact that they have different asymptotic behaviors as $\zeta \rightarrow 0, \infty$ depending on the phase of ζ . In other words, the $b_i[\zeta]$ display Stokes phenomenon, but now in ζ .

In order to set up this Riemann-Hilbert problem, we would like to identify some functions \mathcal{X}_a of the b_i whose asymptotic behavior at small and large ζ is uniform on the whole ζ plane. More concretely, we would like to define the \mathcal{X}_a in such a way that they behave as $\mathcal{X}_a \sim e^{Z_a/\zeta}$ as $\zeta \rightarrow 0$, for all phases of ζ . Here Z_a denotes the four eigenvalues of the connection which go like $Z, -iZ, -Z, iZ$. Of course, due to the Stokes phenomenon in b_i , the price to pay is that there are discontinuities in the $\mathcal{X}_a[\zeta]$ along some rays in the ζ plane. The Riemann-Hilbert problem is captured by the data of such discontinuities. As we will show explicitly below, such discontinuities can be extracted from the various WKB approximations discussed above. One may set up many slightly different Riemann-Hilbert problems, based on slightly different definitions of the \mathcal{X}_a . There is a canonical choice though, inspired by the connection to $\mathcal{N} = 2$ theories in four dimensions [28], which gives discontinuities well suited to formulate the final integral equations we are aiming for.

It is instructive to first consider a non-ideal set of functions Υ_a , allowing for discontinuities at the rays φ_i in order to keep the uniform asymptotics $\Upsilon_a \sim \exp Z_a/\zeta$ uniformly true everywhere. For instance, let us define

$$\begin{aligned} \Upsilon_1[\zeta] &= b_1[\zeta] & \text{for} & \quad -\frac{\pi}{2} < \arg \zeta - \varphi_1 < \frac{\pi}{2} \\ \Upsilon_1[\zeta] &= 1/b_2[\zeta] & \text{for} & \quad \frac{\pi}{2} < \arg \zeta - \varphi_1 < \frac{3\pi}{2} \end{aligned} \tag{3.2}$$

where φ_1 is the phase of Z_1 . We have similar expressions for Υ_2 where we change $b_j \rightarrow b_{j+1}$ and $\varphi_1 \rightarrow \varphi_2 = \varphi_1 - \pi/2$ in the above expression. We then define $\Upsilon_{a+2} = \Upsilon_a^{-1}$. Now, we would like to show that Υ_a has uniform asymptotics. Let us start with Υ_1 . For simplicity, let us set the phase of Z_1 to zero, we will restore it later. In the upper half ζ plane b_3 is very large and we can use (2.27) to write $b_1 b_2 - 1 = b_3^{-1}(b_1 + b_2 + \mu + 1/\mu)$. As b_3 is exponentially larger at small ζ than the factor in parenthesis around the boundary $\arg \zeta = \varphi_1 + \pi/2$ (see fig. 9), we see that $b_2 \sim 1/b_1$. This shows that $1/b_2 \sim \exp[Z_1/\zeta]$ near this line. But since the asymptotics of b_2 is already given by the WKB approximation, we see that this

continues to be true throughout the second sector in (3.2). The same is true for all the Υ_a .

We aim to derive integral equations for the logarithms $\log \Upsilon_a$ from their discontinuities. At this stage, the discontinuities are rather ugly-looking. For example, at $\arg \zeta = \varphi_1 + \pi/2$, Υ_1 goes from b_1 to b_2^{-1} , and the ratio of the two values is a complicated function. This can be easily computed by using the relation (2.27) to write

$$\Upsilon_1(\zeta^+)/\Upsilon_1(\zeta^-) = b_1/b_2^{-1} = b_1 b_2 = 1 + b_3^{-1}(b_1 + b_2 + \mu + \mu^{-1}).$$

Here ζ^\pm denotes arguments for ζ which are slightly bigger or smaller than the discontinuity line. It cannot quite be written as a combination of Υ_a which is continuous on this line. It is always convenient to write the discontinuities in terms of functions where are continuous on that line [28].

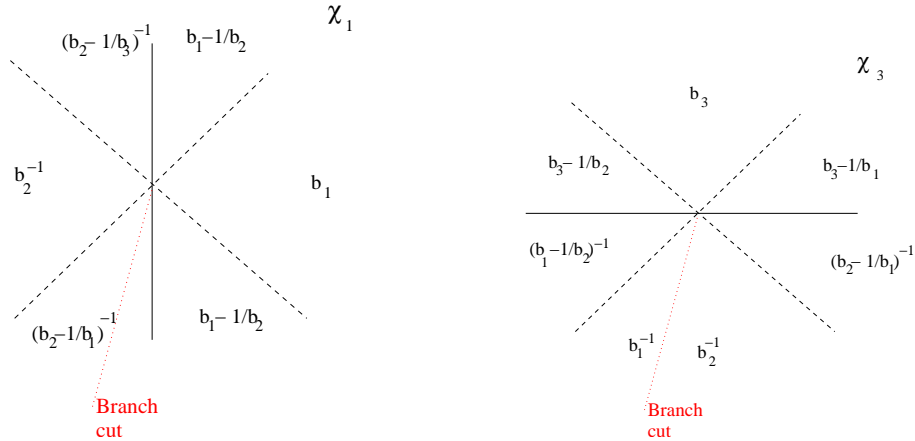


Fig. 10: Here we see the explicit definitions of \mathcal{X}_1 and \mathcal{X}_3 in each angular sector of the ζ plane. (We have set the phase of Z_1 to zero for simplicity). Of course the b_i are discontinuous only at the branch cut. The fact that we define \mathcal{X}_a differently in different sectors is the source of the discontinuities.

We now define new variables \mathcal{X}_a which have simpler discontinuities, although more discontinuity lines. Let us define $\mathcal{X}_a(\zeta)$ to coincide with b_a only for $\varphi_a - \pi/4 < \arg \zeta < \varphi_a + \pi/4$. To define it in the remaining regions we define $\mathcal{X}_a \mathcal{X}_{a-2} = 1$ and also require $\mathcal{X}_a \mathcal{X}_{a-1} = b_a b_{a-1} - 1$ for $\varphi_a < \arg \zeta < \varphi_{a-1}$. The important property of $\mathcal{X}_a \mathcal{X}_{a-1}$ is that its analytic continuation has a simple WKB expression in a sector of angle slightly bigger than π . This defines each \mathcal{X}_a on all the quadrants. In fig. 10 we see the resulting definition of $\mathcal{X}_1, \mathcal{X}_3$. Compared to the variables Υ_a we have now introduced extra discontinuities. The

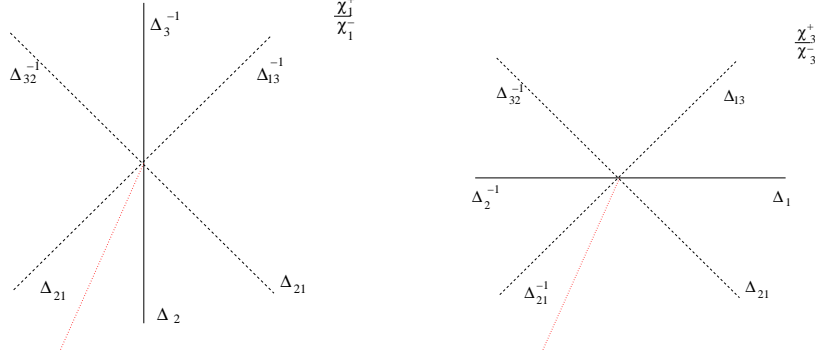


Fig. 11: We see how \mathcal{X}_1 and \mathcal{X}_3 change as we cross the lines of discontinuity. We have defined $\Delta_a = (1 + \mu/\mathcal{X}_a)(1 + \frac{1}{\mu\mathcal{X}_a})$, $\Delta_{a,a-1} = (1 + \frac{1}{\mathcal{X}_a\mathcal{X}_{a-1}})$. These are defined so that, for example, across the top vertical line we have $\mathcal{X}_1^+ = \mathcal{X}_1^- \Delta_3^{-1}$ where \mathcal{X}_1^+ denotes the value of \mathcal{X}_1 just after crossing the line (and \mathcal{X}_1^- just before) if we move in an anti-clockwise fashion.

correction is mild, but important. There are now eight lines of discontinuity. At φ_a , \mathcal{X}_a is continuous. For \mathcal{X}_{a-1} we have the definitions $\mathcal{X}_{a-1} = b_{a-1} - 1/b_a$ and $\mathcal{X}_{a+1} = b_{a+1} - 1/b_a$ on the two sides of the φ_a line. We find

$$\mathcal{X}_{a-1}(\zeta^+)/\mathcal{X}_{a-1}(\zeta^-) = \mathcal{X}_{a-1}(\zeta^+)\mathcal{X}_{a+1}(\zeta^-) = (1 + \mu\mathcal{X}_a^{-1})(1 + \mu^{-1}\mathcal{X}_a^{-1}),$$

where we used (2.27). Hence the discontinuity of $\log \mathcal{X}_{a-1}$ is a function of the continuous variable \mathcal{X}_a : $\log(1 + \mu\mathcal{X}_a^{-1})(1 + \mu^{-1}\mathcal{X}_a^{-1})$. At $\varphi_a + \pi/4$, $\mathcal{X}_a\mathcal{X}_{a-1}$ is continuous by design. For \mathcal{X}_a , we need to compare the definitions $\mathcal{X}_a(\zeta^-) = b_a$ and $\mathcal{X}_a(\zeta^+) = b_a - 1/b_{a-1}$. We find

$$\mathcal{X}_a(\zeta^+)/\mathcal{X}_a(\zeta^-) = 1 - \frac{1}{b_a b_{a-1}} = (1 + \frac{1}{\mathcal{X}_a\mathcal{X}_{a-1}})^{-1}.$$

Hence the discontinuity of $\log x_a$ is a function of the continuous variable $\mathcal{X}_a\mathcal{X}_{a-1}$ only: $-\log(1 + \frac{1}{\mathcal{X}_a\mathcal{X}_{a-1}})$. The resulting discontinuities are summarized in fig. 11.

We have our final Riemann-Hilbert problem: two functions $\log \mathcal{X}_a[\zeta]$, with uniform asymptotic behavior at large and small ζ , and discontinuities which are functions of the \mathcal{X}_a themselves. The discontinuities take the canonical form expected from the connection to $\mathcal{N} = 2$ theories in four dimensions. Indeed, both the asymptotic behavior and the discontinuities of the $\mathcal{X}_a(\zeta)$ are identical to the ones for the cross-ratios of an $SU(2)$ Hitchin system, associated with the $N = 4$ Argyres-Douglas theory in the notation of [29]. The spectral curve for that system takes the form $x^2 = z^4 + U$, which is identical to the curve for the hexagon if one takes $z \leftrightarrow x$. The transformation also relates the canonical differentials xdz , as $xdz + zdx$ is a total derivative. This relation guarantees the coincidence of the periods Z_i , but it does not imply the identity of the discontinuities. That is a non-trivial, and rather unexpected fact.

3.3. An integral equation

Let us first assume that the functions $\mathcal{X}_a[\zeta]$ have no poles or zeros in their region of definition. Along various lines the \mathcal{X}_a will have discontinuities that follow in a simple way from the above definitions. In fig. 11 we have summarized the information about the discontinuities both for \mathcal{X}_1 and \mathcal{X}_3 .

Functions with such discontinuities can be obtained as the solution of integral equations of the form

$$\begin{aligned} \log \mathcal{X}_a &= \frac{Z_a}{\zeta} + \bar{Z}_a \zeta + \\ &+ \sum_b n_{ab} K_{\ell_b} * \log \left(\left(1 + \frac{\mu}{\mathcal{X}_b}\right) \left(1 + \frac{1}{\mu \mathcal{X}_b}\right) \right) + \sum_b m_{ab} K_{\tilde{\ell}_b} * \log \left(1 + \frac{1}{\mathcal{X}_b \mathcal{X}_{b-1}}\right) \\ K_\ell * f &= \frac{1}{4\pi i} \int_\ell \frac{d\zeta'}{\zeta'} \frac{\zeta' + \zeta}{\zeta' - \zeta} f(\zeta'), \\ \ell_j : \frac{Z_b}{\zeta'} &\in R^+, \quad \tilde{\ell}_b : \frac{Z_b + Z_{b-1}}{\zeta'} = (1+i) \frac{Z_b}{\zeta} \in R^+ \end{aligned} \tag{3.3}$$

The Kernels are making sure that when ζ crosses the contour we pick a contribution which is precisely the one we expect for the corresponding discontinuity. The integers n_{ab} , m_{ab} can be read off from figure fig. 11. Namely, for $a = 1$ or $a = 3$ they are the exponents of the Y s in fig. 11. They have the values

$$\begin{aligned} n_{aa} &= 0 & n_{a,a-1} &= -1 & n_{a,a-2} &= 0 & n_{a,a-3} &= 1 \\ m_{aa} &= -1 & m_{a,a-1} &= -1 & m_{a,a-2} &= 1 & m_{a,a-3} &= 1 \end{aligned} \tag{3.4}$$

This equation can be further simplified by using the fact that $\mathcal{X}_{a-1}[i\zeta] = \mathcal{X}_a[\zeta]$ which is due to the Z_4 symmetry of our Hitchin problem. This implies that the values of \mathcal{X}_a that are appearing along the rays ℓ_a are all the same function. Let us set the phase of Z_1 to zero for simplicity. We can then introduce two functions ϵ and $\tilde{\epsilon}$ which parameterize the values of the \mathcal{X}_a and $\mathcal{X}_a \mathcal{X}_{a-1}$ at all the rays. Namely

$$e^{\epsilon(\theta)} \equiv \mathcal{X}_1[\zeta = e^\theta], \quad e^{\tilde{\epsilon}(\theta)} \equiv \mathcal{X}_1 \mathcal{X}_3[\zeta = e^{i\pi/4} e^\theta] \tag{3.5}$$

The functions \mathcal{X}_1 and \mathcal{X}_3 on the full ζ plane can be determined by the two functions of a real variable ϵ and $\tilde{\epsilon}$ through the right hand side of (3.3). The integral equations for ϵ and

$\tilde{\epsilon}$ follow then simply by evaluating the left hand side along the rays used to define ϵ and $\tilde{\epsilon}$. We thus get

$$\begin{aligned}
\epsilon(\theta) &= 2|Z| \cosh \theta + \frac{\sqrt{2}}{\pi} \int d\theta' \frac{\cosh(\theta - \theta')}{\cosh 2(\theta - \theta')} \log(1 + e^{-\tilde{\epsilon}}) + \\
&\quad + \frac{1}{2\pi} \int d\theta' \frac{1}{\cosh(\theta - \theta')} \log(1 + \mu e^{-\epsilon}) \left(1 + \frac{e^{-\epsilon}}{\mu}\right) \\
\tilde{\epsilon}(\theta) &= 2\sqrt{2}|Z| \cosh \theta + \frac{1}{\pi} \int d\theta' \frac{1}{\cosh(\theta - \theta')} \log(1 + e^{-\tilde{\epsilon}}) + \\
&\quad + \frac{\sqrt{2}}{\pi} \int d\theta' \frac{\cosh(\theta - \theta')}{\cosh 2(\theta - \theta')} \log(1 + \mu e^{-\epsilon}) \left(1 + \frac{e^{-\epsilon}}{\mu}\right)
\end{aligned} \tag{3.6}$$

These are completely explicit integral equations for two functions. The integrals run between minus infinity and infinity. The functions ϵ , $\tilde{\epsilon}$ inside the integrals are evaluated at θ' . These turn out to coincide with the TBA equations of the A_3 (or Z_4 symmetric) integrable theory introduced in [30] and further studied in [31]. This theory has two particles of mass m and one bound state with mass $\sqrt{2}m$. A very similar equation was obtained in the study of an x^4 anharmonic oscillator in [14]. Their equation can be obtained by the replacement $|Z| \cosh \theta \rightarrow e^\theta$ which is related to the UV, or conformal, limit of the A_3 theory.

Once we find a solution to (3.6) we can then write the cross ratios, b_i , which we can define through the right hand side of (3.3) and from these we can construct the u_i . Denoting $Z = |Z|e^{i\varphi}$ then note that $b_a[Z, \zeta = 1] = b_a[|Z|, \zeta = e^{-i\varphi}]$. We can pick a definite octant, say $-\pi/4 < \varphi < 0$. We can then compute all three b_i on this octant from the two expressions

$$\begin{aligned}
\log\left(\frac{1}{u_2} - 1\right) &= \log \mathcal{X}_1 \mathcal{X}_3 = 2\sqrt{2} \cos \hat{\varphi} |Z| + \frac{1}{\pi} \int d\theta' \frac{1}{\cosh(\theta' + i\hat{\varphi})} \log(1 + e^{-\tilde{\epsilon}}) + \\
&\quad + \frac{\sqrt{2}}{\pi} \int d\theta' \frac{\cosh(\theta' + i\hat{\varphi})}{\cosh 2(\theta' + i\hat{\varphi})} \log(1 + e^{-\epsilon} \mu) \left(1 + \frac{e^{-\epsilon}}{\mu}\right) \\
\log b_1 &= \log \mathcal{X}_1 = 2|Z| \cos \varphi + \frac{\sqrt{2}}{\pi} \int d\theta' \frac{\cosh(i\varphi + \theta')}{\cosh 2(i\varphi + \theta')} \log(1 + e^{-\tilde{\epsilon}}) + \\
&\quad + \frac{1}{2\pi} \int d\theta' \frac{1}{\cosh(i\varphi + \theta')} \log(1 + e^{-\epsilon} \mu) \left(1 + \frac{e^{-\epsilon}}{\mu}\right)
\end{aligned} \tag{3.7}$$

Where $\hat{\varphi} = \varphi + \pi/4$. From these and (2.27) we can determine

$$\begin{aligned}
b_3 &= \frac{1}{b_1 u_2} \\
b_2 &= \frac{b_1 + b_3 + \mu + \frac{1}{\mu}}{b_1 b_3 - 1}
\end{aligned} \tag{3.8}$$

Once we have defined the b_i on this octant, we can use the symmetries of the problem to map them to other octants. In fact this single octant is a complete solution, since we can always permute the u_i so that we are on this octant.

Notice that the equation we wrote is almost indifferent to the signature. The only difference is that in (3,1) and (1,3) signature μ is a phase, while in (2,2) signature μ is real. The main question one may ask is if the condition on the absence of zeros and poles in the \mathcal{X}_a is self-consistent. There is a regime where the self-consistency is manifest, namely $|U| \gg 1$. In that case the WKB approximation is valid essentially for all ζ , and $\mathcal{X}_a \sim \exp\left[\frac{Z_a}{\zeta} + \bar{Z}_a \zeta\right]$ are such that the logarithms on the right hand side of (3.3) are exponentially small along the contours of integration. In the set up analyzed in [28] this corresponded to a certain “large radius” limit. Thus the problem becomes simple for $|Z| \gg 1$ and it is a good starting point for a numerical solution of the equations. It corresponds to the low temperature limit of the TBA system.

Let us see what large $|U|$, or large $|Z|$, corresponds to in our case. Let us assume that we are in a regime where b_1 and b_3 are both large and have a good WKB approximation. Writing $Z = |Z|e^{i\varphi}$, this corresponds to $-\pi/2 < \varphi < 0$. We then have the expressions

$$\begin{aligned} \log b_1 &\sim 2|Z| \cos \varphi , & \log b_3 &= 2|Z| \cos(\varphi + \frac{\pi}{2}) \\ b_2 &\sim \frac{1}{b_1} + \frac{1}{b_3} \rightarrow u_1 + u_3 \sim 1 , & \frac{u_1}{u_3} &= \frac{b_3}{b_1} \\ u_2 &\sim \frac{1}{b_1 b_3} \ll 1 \end{aligned} \tag{3.9}$$

We see that if the phase φ is generic then we have $(u_1, u_2, u_3) = (1, 0, 0)$ or $(0, 0, 1)$. On the other hand if the phase φ approaches $-\pi/4$ as $|U| \rightarrow \infty$, then we can have a finite value of u_1/u_3 and we get a segment $(1 - u_3, 0, u_3)$, $0 < u_3 < 1$ which joints the two points mentioned above. In other angular sectors we get other segments with $u_i \rightarrow u_{i+1}$.

Thus, the large $|U|$, or large $|Z|$, limit corresponds to cross ratios that are on this triangle. We can move away from this triangle by lowering the value of $|U|$. U , together with μ span the three dimensional space of cross ratios u_i . Within this space there will be solutions that can be interpreted as living in various signatures. In the next subsection we describe more precisely the region in the space of cross ratios which is spanned by polygons living in space with various signatures.

3.4. Kinematics, signature and the space of cross ratios

In this section we discuss the kinematics relevant for the hexagonal Wilson loop (or scattering of six particles), in several signatures. We consider an hexagon with cusps at points x_i in four dimensions, such that the distance between two consecutive points is light-like. One can construct three independent cross-ratios

$$u_1 = \frac{x_{13}^2 x_{46}^2}{x_{14}^2 x_{36}^2}, \quad u_2 = \frac{x_{24}^2 x_{15}^2}{x_{25}^2 x_{14}^2}, \quad u_3 = \frac{x_{35}^2 x_{26}^2}{x_{36}^2 x_{25}^2} \quad (3.10)$$

we would like to understand the range of such cross-ratios in different signatures, namely, (3, 1), (2, 2) and (1, 3). It is convenient go to a conformal frame where we have sent three points, for instance $x_{6,1,5}$, to infinity. Furthermore, we set the position of x_3 as the origin. To be more specific, we denote four dimensional coordinates by $x = (x^+, x^-, x_\perp)$ and choose

$$\begin{aligned} x_3 &= (0, 0, 0), & x_2 &= (-1, x_2^-, \vec{p}), & x_4 &= (x_4^+, -1, \vec{q}) \\ x_1 &= x_2 + (0, \Lambda, 0), & x_5 &= x_4 + (\Lambda, 0, 0), & x_6 &= (\Lambda, \Lambda, 0) + \dots \end{aligned} \quad (3.11)$$

Since x_2 and x_4 are light-like vectors, we require $x_2^- = -\vec{p}^2$, $x_4^+ = -\vec{q}^2$. Here, \vec{p} and \vec{q} are two vectors living in the transverse space. This transverse space has various signatures. They can be used to write the cross ratios.

$$u_1 = \frac{1}{1 - \vec{q}^2}, \quad u_2 = \frac{1 + \vec{q}^2 \vec{p}^2 - 2\vec{q} \cdot \vec{p}}{(1 - \vec{q}^2)(1 - \vec{p}^2)}, \quad u_3 = \frac{1}{1 - \vec{p}^2}, \quad (3.12)$$

The regular hexagon embedded in AdS_3 corresponds to $\vec{q} = \vec{p} = 0$, with $u_i = 1$. We are interested in solutions continuously connected with the regular hexagon, for which $u_i > 0$. A negative sign for some u_i means that some of the distances between cusps are becoming timelike. In this paper we will discuss only the case where the $u_i \geq 0$ where distances are not yet timelike.

Let us discuss in more detail the physical meaning of the large $|U|$ lines, for example $u_2 = 0$, $u_1 + u_3 = 1$. The second condition sets $\vec{q}^2 \vec{p}^2 = 1$. Since, u_i are positive, we see that u_1, u_3 are less than one. This means that \vec{q}^2 and \vec{p}^2 are negative. The condition $u_2 = 0$ requires $\vec{p} \cdot \vec{q} = 1$, which implies that \vec{p} and \vec{q} are collinear and point in opposite directions. We see then that the four dimensional vectors x_2 and x_4 are collinear as well. We conclude that the large $|U|$ regime is actually the collinear limit. In fact, the fraction $z = \frac{k_{23}^\mu}{k_{23}^\mu + k_{34}^\mu} = u_1$, where the $k_{i,i+1} = x_{i+1} - x_i$ are the spacetime momenta. Thus, as we move along the segment $(1 - u_3, 0, u_3)$ we change this fraction which is a free parameter in

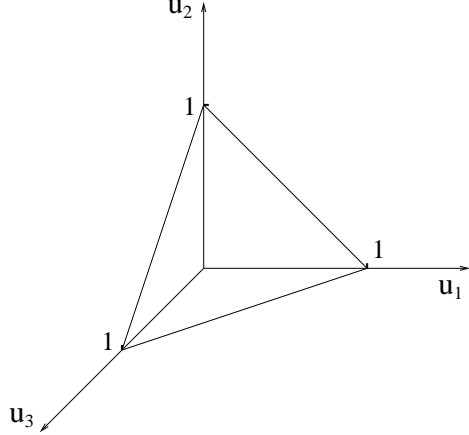


Fig. 12: This is the three dimensional space of cross ratios parameterized by (u_1, u_2, u_3) . The lines belonging to the edges of the triangle correspond to the large $|U|$ limit. These edges correspond to various collinear limits. The vertices of the triangles correspond to soft limits.

the collinear limit. Note that for z to be different from zero or infinity we need to fine-tune the phase of $|U|$ as we move to large values of $|U|$. However, in this regime the area, A_{free} is not sensitive to this phase. In fact, we will see that our remainder function remains constant in this limit. Taking the large $|U|$ limit along a generic direction gives us a simple soft limit which simply eliminates one of the momenta. Let's say that $u_3, u_1 \rightarrow 0$ in this limit, then we conclude that $\vec{q}^2 \rightarrow \infty$, which after a rescaling, is making $x_2 \sim x_3$. Thus, we are sending the momentum $k_{23} \rightarrow 0$.

Note that the expressions (3.12) are valid for any signature under consideration. Of course, the sign of \vec{q}^2 depends on the signature. For instance, for $(3, 1)$ signature, $\vec{q}^2 \geq 0$ and hence $u_i > 1$, while for $(1, 3)$ signature, $\vec{q}^2 < 1$ and $u_i < 1$. However, the converse is not true. The reason is simple, with $(2, 2)$ signature we can have either sign for \vec{q} .

To get more information we look at the sign of $\vec{p}^2 \vec{q}^2 - (\vec{p} \cdot \vec{q})^2$, which is positive in $(3, 1)$ and $(1, 3)$, but is negative in $(2, 2)$. This can be translated into a condition on μ . Combining (2.27) with (3.10) we can write μ as

$$\mu + \mu^{-1} = \frac{1 - u_1 - u_2 - u_3}{\sqrt{u_1 u_2 u_3}} \quad (3.13)$$

Using the above formulas we can write

$$-\frac{1}{4}(\mu - \mu^{-1})^2 = \frac{u_1 u_3}{u_2} \left(\vec{p}^2 \vec{q}^2 - (\vec{p} \cdot \vec{q})^2 \right) \quad (3.14)$$

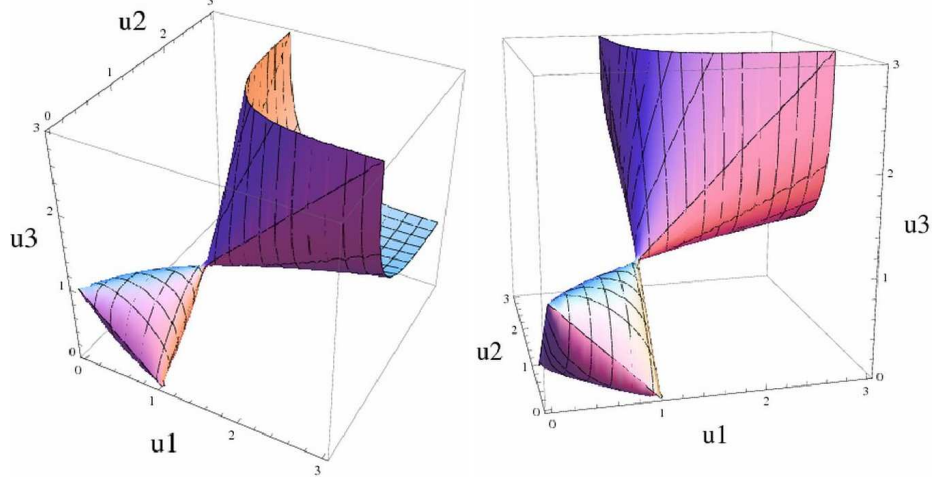


Fig. 13: Here we see the AdS_4 surface corresponding to $\mu = \pm 1$ in the space of cross ratios parametrized by (u_1, u_2, u_3) . Points on this surface corresponds to cross ratios that arise when we have a polygonal contour in a three dimensional space. The surface pinches at $u_i = 1$. The region inside the “bag” in the $u_i < 1$ region correspond to configurations in $(1, 3)$ signature. The region outside corresponds to surfaces in $(2, 2)$ signature. Finally the region inside the surface for $u_i > 1$ corresponds to ordinary $(3, 1)$ signature. We show the same surface from two different viewing directions.

We conclude that μ is a phase for $(3, 1)$ and $(1, 3)$ but μ is real for $(2, 2)$. Thus the boundary of the $(2, 2)$ signature lies at $\mu = \pm 1$. These values coincide with the ones corresponding to surfaces that can be embedded in AdS_4 . This is not surprising, we need to make one spacetime coordinate vanish if we are going to change its signature. We plot this surface in fig. 13. The surface pinches at $u_1 = u_2 = u_3 = 1$. This corresponds to the regular hexagon embedded in AdS_3 , all three signatures meet here. The AdS_4 surface has two sheets emanating from the large $|U|$ triangle. One sheet has $\mu = -1$, it starts at the large $|U|$ triangle, goes through the pinch at $u_i = 1$ and then continues through to $u_i > 1$. The other has $\mu = 1$ and it stays at $u_i < 1$. It has the topology of a disk and it contains an interesting polygon with $u_1 = u_2 = u_3 = \frac{1}{4}$. This is another kind of regular hexagon which has a simple picture in $(2, 2)$ signature and it is discussed further in appendix B. These two branches together define the full AdS_4 surface. The region inside the surface for $u_i < 1$ has $(1, 3)$ signature, the region outside has $(2, 2)$ signature and the region inside for $u_i > 1$ corresponds to ordinary $(3, 1)$ signature.

It is interesting to look at the surfaces of constant μ which end on the large radius triangle. We have already discussed the $\mu = \pm 1$ surfaces. If μ is a phase the surface has the topology of a disk which sits in the $(1, 3)$ signature region (one space three times). We

expect that as we solve the integral equation for decreasing values of $|U|$ starting from the large radius region, we will get a nice map from the U plane covering the disk once. It turns out that $U = 0$ corresponds to the line $u_1 = u_2 = u_3$. We move along the line by changing μ . In section five we find the exact solution corresponding to this case.

If we take μ to be real and negative, the surface has the topology of a cylinder in the region $u_i > 0$, and has some pieces in the regions with some u_i negative. We expect that as one moves towards small $|U|$, it will cover the cylinder, and then at some point one b_a will become negative, making two u_i negative. In order to reach the $(3, 1)$ signature region, a possible strategy is to solve the integral equation starting from the large radius region, with μ real and slightly smaller than -1 , follow it until we get to the $u_i > 1$ region, and then cross into the $3, 1$ signature by changing μ back to a phase. Some interesting phenomena can occur in the process, if the functions $\mathcal{X}_a[\zeta]$ acquire zeroes or poles. This is a common (even desirable at times) occurrence in solving TBA-like equations [32,33]. In appendix C we discuss this a bit further.

4. Area and TBA free energy

In this section we will show how to compute a certain regularized area as the free energy of the TBA system for the hexagon case.

The area is given by $2 \int e^\alpha$ which is divergent. This should be regularized in a physical way. For the time being let us just define a regularized version by subtracting the behavior of e^α far away. We have seen that $\hat{\alpha}$ (2.19) goes to zero at infinity. This means that for large z , $e^\alpha \sim |P|^{1/2}$. Furthermore, in the case of the hexagon, we also have that $|P|^{1/2} \sim |z|$ at infinity. Thus we find it convenient to introduce the following definitions

$$\begin{aligned}
A_{reg} &= A_{periods} + A_{free} = 2 \int d^2(e^\alpha - |z|) \\
A_{periods} &\equiv 2 \int d^2 z (|P(z)|^{1/2} - |z|) = |Z|^2 \\
A_{free} &\equiv 2 \int d^2 z (e^\alpha - |P|^{1/2})
\end{aligned} \tag{4.1}$$

where we have evaluated explicitly $A_{periods}$ in terms of (3.1). Note that this is a convergent integral in our case since $P(z) = z^2 - U$.

It is convenient to write A_{reg} in terms of the ‘‘Higgs’’ fields of the Hitchin system using

$$Tr \Phi_z \Phi_{\bar{z}} = e^\alpha - v^I \bar{v}_I e^{-\alpha} = 2e^\alpha - \partial \bar{\partial} \alpha$$

Hence, up to a total derivative which integrates to πN , we can define (the trace is in the spinor representation)

$$A_{free} = \int d^2z [Tr \Phi_z \Phi_{\bar{z}} - 2|z|] d^2z$$

The formal expression $\int Tr \Phi_z \Phi_{\bar{z}}$ has a nice interpretation in the context of the Hitchin system. Recall there is a natural Poisson bracket on functionals of A, Φ

$$\{U, V\} = \frac{i}{2} \int d^2z Tr \left[\frac{\delta U}{\delta \Phi_z} \frac{\delta V}{\delta \Phi_{\bar{z}}} + \frac{\delta U}{\delta A_z} \frac{\delta V}{\delta A_{\bar{z}}} - (z \leftrightarrow \bar{z}) \right] \quad (4.2)$$

and the flow generated by $\int Tr \Phi_z \Phi_{\bar{z}}$ rotates Φ_z and $\Phi_{\bar{z}}$ in opposite directions as $\delta \Phi_z = \frac{i}{2} \Phi_z$, $\delta \Phi_{\bar{z}} = -\frac{i}{2} \Phi_{\bar{z}}$

The Poisson bracket is gauge invariant, and it actually descends to a nice Poisson bracket on functionals of the flat sections of the spectral connection, such as the b_i . On such functionals, it reduces to

$$\{U, V\} = i \int d^2z Tr \left[\frac{\delta U}{\delta \mathcal{A}_z} \frac{\delta V}{\delta \mathcal{A}_{\bar{z}}} - (z \leftrightarrow \bar{z}) \right] \quad (4.3)$$

It is straightforward, but tedious, to compute the Poisson bracket $\{b_i, b_{i-1}\} = b_i b_{i-1} - 1$ along the lines of appendix B of [29]. There is a self-consistency check, one can see that $\{b_i[\zeta], b_{i-1}[\zeta]\}$ had to be some polynomial in the $b_i[\zeta]$ with constant coefficients independent of ζ . The right hand side $b_i b_{i-1} - 1$ is the only possibility consistent with the asymptotics of b_i at small ζ along all the rays in the ζ plane. Also, $\{b_i, \mu\} = 0$. Another consistency check is that this Poisson bracket is consistent with the relation (2.27). Taking the Poisson bracket of the two sides of (2.27) with b_1 we get

$$\{b_1, b_1 b_2 b_3\} = b_1 b_2 (b_1 b_3 - 1) - b_1 (b_1 b_2 - 1) b_3 = b_1 b_3 - b_1 b_2 = \{b_1, b_1 + b_2 + b_3 + \mu + \mu^{-1}\}.$$

Finally, the neatest result: $\{\mathcal{X}_a, \mathcal{X}_{a-1}\} = \mathcal{X}_a \mathcal{X}_{a-1}$ identically in all sectors. In particular, the discontinuities in the $\mathcal{X}_a[\zeta]$ preserve the Poisson bracket, and the corresponding symplectic form

$$\omega = d \log \mathcal{X}_1 d \log \mathcal{X}_3 = d \log \mathcal{X}_1 d \log(\mathcal{X}_1 \mathcal{X}_3) .$$

The asymptotic behavior of \mathcal{X}_a at $\zeta = 0, \infty$ shows that ω holomorphic in ζ everywhere, and hence is ζ independent.

A rotation of Φ_z and $\Phi_{\bar{z}}$ in opposite directions can be absorbed by a phase rotation of ζ . Can we identify a function F which can generate this phase rotation directly? It should satisfy the equation

$$dF = \frac{i}{2} [d \log \mathcal{X}_1 \zeta \partial_\zeta \log \mathcal{X}_3 - d \log \mathcal{X}_3 \zeta \partial_\zeta \log \mathcal{X}_1] . \quad (4.4)$$

F , as ω , will be ζ independent. This allows us to compute it at, say, very small ζ . From the integral equation, we can extract the behavior of $\log x_a$ at small ζ

$$\log \mathcal{X}_a \sim \frac{Z_a}{\zeta} + K_a + \zeta (\bar{Z}_a + K'_a) \quad (4.5)$$

Here K_a and K'_a are simply the value at $\zeta = 0$ and the first derivative at $\zeta = 0$ of the convolution terms in the integral equation. Then

$$\zeta \partial_\zeta \log \mathcal{X}_a \sim -\frac{Z_a}{\zeta} + \zeta (\bar{Z}_a + K'_a)$$

and dF can be written as $dF = dF_1 + dF_2$ where

$$dF_1 = \frac{i}{2} d(Z_1 \bar{Z}_3 - \bar{Z}_1 Z_3) = d|Z|^2 \quad (4.6)$$

where we used that $Z_1 = Z$ and $Z_3 = iZ$. This is the dominant contribution in the large $|Z|$ limit. The second term is

$$dF_2 = \frac{i}{2} d(Z_1 K'_3 - Z_3 K'_1) \quad (4.7)$$

F_2 can be rearranged a little, to the form

$$F_2 = \frac{1}{4\pi} \int_{\ell_a} \frac{d\zeta'}{\zeta'} \frac{Z_a}{\zeta'} \log \left(\left(1 + \frac{\mu}{\mathcal{X}_a}\right) \left(1 + \frac{1}{\mu \mathcal{X}_a}\right) \right) + \frac{1}{4\pi} \int_{\tilde{\ell}_a} \frac{d\zeta'}{\zeta'} \frac{Z_a + Z_{a-1}}{\zeta'} \log \left(1 + \frac{1}{\mathcal{X}_a \mathcal{X}_{a-1}}\right) \quad (4.8)$$

A similar calculation at large ζ produces a similar result, but with $\frac{Z_a}{\zeta'}$ replaced by $\bar{Z}_a \zeta'$. The two expressions must be identical, and we can take the average

$$F_2 = \frac{1}{8\pi} \int_{\ell_a} \frac{d\zeta'}{\zeta'} \left(\frac{Z_a}{\zeta'} + \bar{Z}_a \zeta' \right) \log \left(\left(1 + \frac{\mu}{\mathcal{X}_a}\right) \left(1 + \frac{1}{\mu \mathcal{X}_a}\right) \right) + \frac{1}{8\pi} \int_{\tilde{\ell}_a} \frac{d\zeta'}{\zeta'} \left(\frac{Z_a + Z_{a-1}}{\zeta'} + (\bar{Z}_a + \bar{Z}_{a-1}) \zeta' \right) \log \left(1 + \frac{1}{\mathcal{X}_a \mathcal{X}_{a-1}}\right) \quad (4.9)$$

Notice that F_2 goes to zero in the large $|Z|$ limit. In this limit the dominant piece is F_1 , which reproduces $A_{periods}$. Note that there could have been a μ dependent integration

constant in F . However, this is not the case because we know from the properties of the solutions that A_{free} as defined in (4.1) goes to a constant for large $|Z|$. Thus the conclusion is that, up to a constant, we have that $A_{free} = F_2$. Finally, let us write A_{free} in terms of the solutions of the integral equation (3.7)

$$A_{free} = \frac{1}{2\pi} \int_{-\infty}^{\infty} d\theta 2|Z| \cosh \theta \log(1 + e^{-\epsilon} \mu) \left(1 + \frac{e^{-\epsilon}}{\mu}\right) + 2\sqrt{2}|Z| \cosh \theta \log(1 + e^{-\tilde{\epsilon}}) \quad (4.10)$$

This has precisely the form of the free energy (up to an overall sign) of the TBA system in (3.6).

In order to get the full physical answer of the problem we need to introduce a more physical regulator. The physical regulator consists in cutting off the integral when the radial AdS coordinate gets too close to the boundary. If z is the radial AdS_5 coordinate we say that $z > \epsilon_c$. Here ϵ_c is a short distance UV cutoff from the Wilson loop perspective or an IR scale from the amplitude point of view. Thus we are cutting off the z integral in a way that depends on the solution. However, this dependence on the solution can be expressed in terms of the distances between the cusps (it depends on distances, not only on cross ratios). We explain this in detail in the appendix. We find that

$$A = A_{div} + A_{BDS-like} + A_{periods} + A_{free} + \text{constant} \quad (4.11)$$

where A_{div} contains the ϵ_c dependent divergent terms. $A_{BDS-like}$ is finite but it depends on physical distances and not just the cross ratios. Its explicit form is given in appendix A. It obeys the anomalous conformal symmetry Ward identities derived in [34]. It has become conventional to define a remainder function by subtracting the specific function A_{BDS} given in [35], which has the functional form of the one loop result. Thus one defines a remainder function via

$$\begin{aligned} R &\equiv -(A - A_{div} - A_{BDS}) = -(A_{BDS-like} - A_{BDS}) - A_{periods} - A_{free} + \text{constant} \\ R &= \sum_{i=1}^3 \left(\frac{1}{8} \log^2 u_i + \frac{1}{4} Li_2(1 - u_i) \right) - |Z|^2 - A_{free} + \text{constant} \end{aligned} \quad (4.12)$$

In the large $|Z|$ limit, which is the collinear limit, one can check using (3.9) that the first term in R , involving u_i , cancels the $|Z|^2$ term, up to a constant. Thus the remainder function goes to a constant in the large $|Z|$ limit, since $A_{free} \rightarrow 0$ in this limit. As argued

in [35], the A_{BDS} term gives the expected result in the collinear limit. Thus, the remainder function should be finite. This is a simple check of our results.

Let us summarize the final result. The objective is to find the remainder function R as a function of the spacetime cross ratios u_i . For this purpose, we compute μ from the u_i via (3.14) and we introduce an auxiliary complex parameter Z . We then solve the integral equations (3.6) and determine the functions $\epsilon(\theta)$, $\tilde{\epsilon}(\theta)$. These functions depend on the parameters $|Z|$ and μ . We then solve for the spacetime cross ratios u_i (or equivalently b_i (3.10)) using (3.7), (3.8). *In principle*, one would be able to invert that relation and compute Z and μ in terms of the spacetime cross ratios u_i . Finally, one can compute A_{free} as a function of $|Z|$ and μ using (4.10) and insert the result in (4.12). In practice one can numerically compute the functions ϵ , $\tilde{\epsilon}$, the u_i and the area as a function of $|Z|$ and μ .

5. Analytic solution of the integral equation

In the following we will compute the area from the integral equation in the particular limit $U \rightarrow 0$. This corresponds to the special kinematical configurations with $u_1 = u_2 = u_3 = u$. From the point of view of the TBA equations this limit corresponds to a high temperature/conformal limit and has been analyzed for instance in [36,37] (see also [38,39,40]) to which we refer the reader for the details. We start by recalling the general result in these references and then we focus on the specific case at hand. Consider the standard form of TBA equations

$$\epsilon_a(t) = m_a \cosh t - \sum_b \int \frac{dt'}{2\pi} K_{ab}(t-t') \log(1 + \lambda_b e^{-\epsilon_b(t')}) \quad (5.1)$$

where the indices a, b run over different species, m_a denote their masses and λ_a their chemical potential. Then, the free energy of the system can be written as

$$F = - \sum_a \frac{m_a}{2\pi} \int dt \cosh t \log(1 + \lambda_a e^{-\epsilon_a(t)}) \quad (5.2)$$

It turns out that the free energy can be exactly computed in this limit [36,37,38,39]

$$F(m_a \rightarrow 0) = -\frac{1}{\pi} \sum \mathcal{L}_{\lambda_a}(x_a), \quad \mathcal{L}_\lambda(x) = \frac{1}{2} \left(\log x \log(1 + \frac{\lambda}{x}) - 2Li_2 \left(-\frac{\lambda}{x} \right) \right) \quad (5.3)$$

The parameters x_a are the solution of the system of equations

$$x_a = \prod_b \left(1 + \frac{\lambda_b}{x_b} \right)^{N_{ab}}, \quad N_{ab} = -\frac{1}{2\pi} \int_{-\infty}^{\infty} dt K_{ab}(t) \quad (5.4)$$

Note that the final result does not depend much on the details of the Kernels (only their integrals)

5.1. Particular case at hand

The integral equations (3.6) are exactly in the standard form (5.1), so that we can apply the above results straightforwardly. We have three species of particles, that we call ϵ_1 , ϵ_2 and $\tilde{\epsilon}$ (with $\epsilon_1 = \epsilon_2 = \epsilon$). The mass of each excitation is ⁹

$$m_{\tilde{\epsilon}} = \sqrt{2}|Z|, \quad m_{\epsilon_1} = m_{\epsilon_2} = |Z| \quad (5.5)$$

The chemical potential for each species is $\lambda_{\tilde{\epsilon}} = 1$, $\lambda_{\epsilon_1} = \mu$ and $\lambda_{\epsilon_2} = 1/\mu$. From the particular kernels in our equation (3.6) we can easily compute N_{ab} . We find

$$N_{\tilde{\epsilon}\tilde{\epsilon}} = 1, \quad N_{\tilde{\epsilon}\epsilon_i} = N_{\epsilon_i\tilde{\epsilon}} = 1, \quad N_{\epsilon_i\epsilon_j} = \frac{1}{2} \quad (5.6)$$

Plugging this in (5.4), we can solve for $x_{\tilde{\epsilon}}$ and $x_{\epsilon} = x_{\epsilon_1} = x_{\epsilon_2}$, we find

$$e^{\tilde{\epsilon}} = x_{\tilde{\epsilon}} = 1 + \mu^{2/3} + \mu^{-2/3}, \quad e^{\epsilon} = x_{\epsilon} = \mu^{1/3} + \mu^{-1/3} \quad (5.7)$$

The free energy is simply

$$F = -\frac{1}{\pi} (\mathcal{L}_1(x_{\tilde{\epsilon}}) + \mathcal{L}_{\mu}(x_{\epsilon}) + \mathcal{L}_{1/\mu}(x_{\epsilon})) \quad (5.8)$$

Using the explicit expression for \mathcal{L} and identities involving di-logarithms one can show the very simple result

$$-F = A_{free} = \frac{\pi}{6} - \frac{1}{3\pi}\phi^2, \quad \mu = e^{i\phi} \quad (5.9)$$

Several comments are in order. First, is it possible to solve numerically the integral equation for small values of Z (for instance $Z = 0.01$). After several iterations we find numerical results that are in perfect agreement with the analytic solution (5.9), see for instance the following figure

⁹ Quite interestingly, note that the mass of these three excitations agree (up to the proportionality factor $|Z|$) with the masses of the three fluctuations around the classical string solution describing a single cusp (or four cusps) in AdS_5 , see [41].

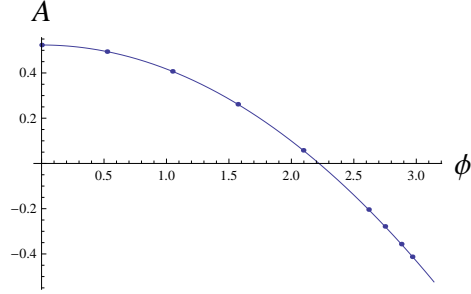


Fig. 14: Analytic (continuous line) vs. numeric (points) solutions of the integral equation for the case $Z = 0.01$ and $\mu = e^{i\phi}$, with ϕ running from 0 to π .

In particular, this shows that the numerical solutions can be quite reliable.

Second, we see that the values of the regularized area/free energy for $\mu = \pm 1$ is simply given by $\pm \frac{\pi}{6}$. This values of μ correspond to $u = 1/4$ and $u = 1$ respectively, and the value for the free energy is in very good agreement with what we expect from the numerical analysis of appendix B.¹⁰ Recall that $\mu = \pm 1$ corresponds to the two kinds of regular hexagons.

Third, the free energy can be expressed in terms of u by using

$$\mu + \mu^{-1} = 2 \cos \phi = \frac{1 - 3u}{u^{3/2}} \quad (5.10)$$

where ϕ is not necessarily real. We are interested in the whole region $u > 0$. We can cover this region by going along the following contour in the μ -plane

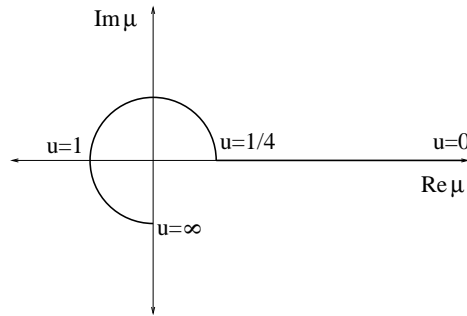


Fig. 15: Different values of u as we follow the path shown by the figure in the μ -plane. For $u > 1/4$ μ is a phase.

¹⁰ The subtraction of $2A_{pentagon}$ in appendix B is needed since the free energy was defined in such a way that is zero for very large values of $|Z|$.

As μ is real and very large, u is very close to zero. As we approach $\mu = 1$, u grows until $u = 1/4$ at $\mu = 1$. For $u > 1/4$, μ is a phase, with $\mu = -1$ at $u = 1$ and u becoming very large as μ approaches $-i$.

The final answer for the remainder function in this regime is then obtained by adding up all the contributions

$$R(u, u, u) = -\frac{\pi}{6} + \frac{1}{3\pi}\phi^2 + \frac{3}{8}(\log^2 u + 2Li_2(1-u)), \quad u = \frac{1}{4\cos^2(\phi/3)} \quad (5.11)$$

This is the remainder function for the scattering of six gluons at strong coupling in the particular kinematical configuration in which all the cross-ratios u_i coincide.

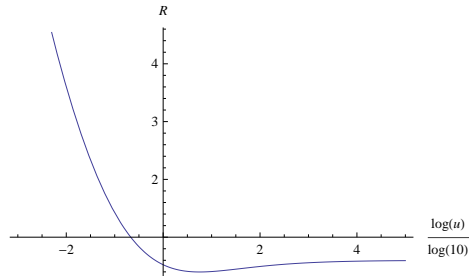


Fig. 16: Remainder function (5.11) at strong coupling for $u_1 = u_2 = u_3 = u$

5.2. A curious observation

The remainder function at two loops for the case at hand was extensively considered in [42], based on previous work [13,12,43]. In that paper the remainder function was computed numerically for several values of u (in particular, $u = 1/9, 1/4, 1, 3.83$ and $u = 100$). We could try to fit their numerics by a function with some arbitrary coefficients but the general structure of (5.11), similar to what it was done in [44] for the case of the octagon in AdS_3 . More precisely, we consider a function of the form

$$R_{c_1, c_2, c_3} = c_1 \left(-\frac{\pi}{6} + \frac{1}{3\pi}\phi^2 \right) + c_2 \frac{3}{8}(\log^2 u + 2Li_2(1-u)) + c_3 \quad (5.12)$$

The idea is that the high temperature of the TBA equations are not too sensitive to the precise form of the kernels, so that perhaps this functional form holds for all values of the coupling. In addition, in our computation, the two terms arise in a somewhat independent fashion, so we have given us the freedom to change their relative coefficients¹¹. It turns out that for certain values of c 's, namely $c_1 \approx 12.2$, $c_2 \approx 11.4$, $c_3 \approx -9.1$, we get a quite good approximation of the two loops result, see the following figure

¹¹ Note that we obtain that $c_1/c_2 \approx 1.07$, which is close to one, so perhaps we should not change the relative coefficients of the two terms!

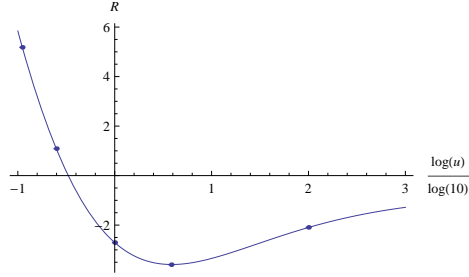


Fig. 17: R_{c_1, c_2, c_3} (continuous line) vs. numerical values (points) for the remainder function at two loops

However, the asymptotic value for R as $u \rightarrow \infty$ seems slightly higher than the value computed in [42]. It would be interesting to try to understand better the two loops result in this particular regime. In particular, it would be interesting to find its analytical expression and compare it with the strong coupling result.

Comparing the two loops (figure 8 of [42]) and strong coupling results, we see that many qualitative features are very similar and are probably independent on the coupling. For instance, the apparently universal behavior $R \approx h(\lambda) \log^2 u$ for small u may be simple to understand and $h(\lambda)$ may be computable for all λ .

After the first version of this paper was published, an analytic expression for the two loop result was found [45]. The function looks very similar to the strong coupling result, but it *cannot* be fitted by an ansatz of the form (5.12).

6. Conclusions

In this paper we have studied minimal surfaces in AdS_5 . These are the classical solutions for strings moving in AdS_5 . We have shown that the problem can be mapped into an $SU(4)$ Hitchin problem. More precisely, it is a Z_4 projection of an $SU(2, 2)$ Hitchin problem. An important observation is the existence of a spin four holomorphic current $P(z)$ on the worldsheet. For surfaces that end on a polygonal contour, P is a polynomial whose degree depends on the number of sides of the polygon. In the Hitchin language we have an essential singularity at $z = \infty$. This singularity has its associated Stokes phenomenon. This Stokes phenomenon is important for the emergence of the polygon on the boundary of AdS . In fact, the shape of the polygon is related to the Stokes matrices of the solutions of the flat Hitchin connection. The shape of the polygon is encoded in the coefficients of the polynomial as certain phases which correspond to other moduli of the Hitchin system.

The integrability of the Hitchin equations can be used to analyze this problem. We introduced the parameter ζ and studied the problem as a function of ζ . When ζ is a phase, we have the ordinary physical problem, but with complex ζ it is some sort of deformation of the physical problem. The nice feature is that for $\zeta \rightarrow 0$ or $\zeta \rightarrow \infty$ one can solve it using a simple WKB approximation. This solution displays a Stokes-like phenomenon but now in the ζ plane. The Stokes “factors” can be found explicitly by analyzing the small ζ problem. Given that we have an analytic function of ζ (analytic away for $\zeta =, \infty$) with given Stokes-like behavior at zero or infinity, we can recover the function. This is done by first formulating a Riemann-Hilbert problem and then writing its associated integral equation.

Surprisingly, this integral equation (3.6) has the form of a TBA equation with rather simple kernels. In fact, they are the TBA equations for an A_3 (or Z_4) theory discussed in [30,38]. The area coincides with the free energy of the TBA system.

The TBA equation can be solved rather simply by a numerical iterative process. The TBA equation depends on two parameters $|Z|$ and μ (3.6). The non-trivial part of the area, which is the free energy of the TBA, also depends on $|Z|$ and μ (4.10). Once the solution is found we can determine the spacetime cross ratios, u_1, u_2, u_3 , in terms of Z and μ (3.7)(3.8). This leads to the final result for the remainder function (4.12).

There is a special set of cross ratios $u_1 = u_2 = u_3$ for which the problem simplifies. This corresponds to the high temperature limit of the TBA. This limit was studied in [38,36]. Using these results we could find an explicit, and rather simple, analytic expression for the full answer (5.11).

For us, the connection to the TBA system was an “experimental” observation. It would be nice to find a simple argument leading more directly to this TBA equation. It is interesting that the TBA that we found corresponds to the A_3 theory [30,38], which is associated to $SU(4)$, the group associated to the Hitchin equations¹².

Extending the techniques used in this paper to the case of more gluons should be straightforward. We expect that we will end up with a more complicated pattern of discontinuity lines in the ζ plane. We expect that the lines will organize in groups of four lines at right angles, but with different groups rotated with respect to each other. The

¹² Note that the spectrum of particles in the A_3 integrable theory [30,38], two particles of mass m and one particle of mass $\sqrt{2}m$ coincides precisely with the spectrum of particles for small fluctuations around the string worldsheet describing a single cusp, analyzed in [41].

TBA will have a similar structure, probably with one unknown function per group of four lines. But the final area is still given by the free energy of this TBA system.

One would also like to generalize these results to the full quantum problem. It is natural to imagine that perhaps the full quantum answer is also given by a TBA equation involving the same particles but with a different kernel which includes all quantum corrections. Or perhaps we have a similar kernel but a different mapping between the parameters Z and μ of the integral equations with the spacetime cross ratios. A natural next step would be to extend the Pohlmeyer reduction and the relation to the Hitchin equations for the full $PS(2,2|4)$ supercoset theory. This should make it clear how to compute N^k MHV amplitudes.

The large temperature limit of the TBA calculation is insensitive to the precise form of the kernel. What is important is the total integral of the kernel (5.4). Thus, one can speculate that perhaps for all values of the coupling one has a form similar to the one we found, but perhaps with a different coefficient (5.12). In fact, if one allows for general coefficients, the functional form that we found is very close.

7. Acknowledgments

We thank N. Arkani-Hamed and F. Cachazo for discussions.

This work was supported in part by U.S. Department of Energy grant #DE-FG02-90ER40542.

Appendix A. Regularization of the area

In this appendix we regularize the area using a physical cutoff which is appropriate to regularize the Wilson loop or the amplitude. The idea is very similar to the one used in [25]. For the sake of completeness we give a brief description. The story is relatively simple in the case that the number of gluons is not a multiple of four, $n \neq 4k$. We will treat only this case here, since we mainly deal with the $n = 6$ case which certainly obeys this condition ¹³.

¹³ The case where $n = 4k$ was treated explicitly in [25] for AdS_3 kinematics. We expect similar results for generic AdS_5 kinematics.

The area can be written as

$$\begin{aligned}
A &= A_{\text{free}} + A_{\text{periods}} + A_{\text{cutoff}} \\
A_{\text{free}} &= 2 \int d^2 z [e^\alpha - (P\bar{P})^{1/4}] \\
A_{\text{periods}} &= 2 \int_{\Sigma} d^2 z (P\bar{P})^{1/4} - 2 \int_{\Sigma_0} d^2 w = 2 \int_{\Sigma} d^2 w - 2 \int_{\Sigma_0} d^2 w \\
A_{\text{cutoff}} &= 2 \int_{\Sigma_0, Y^+ > 1/\epsilon_c} d^2 w
\end{aligned} \tag{A.1}$$

Where A_{free} is the non-trivial function that is computed as the free energy of the TBA equation (4.9) for the case of $n = 6$. In the definition of A_{periods} we have used that the polynomial P defines a surface Σ which is the w plane with the appropriate cuts. We have introduced Σ_0 as a reference surface with a single branch point at the origin and the same structure at infinity. In order to subtract the two it is very important to regularize both computations with a cutoff in the w plane, such as $|w| = \Lambda \gg 1$, but not a cutoff in the z plane. Using this cutoff for defining the difference in A_{periods} we find that it can be explicitly evaluated in terms of periods on the Riemann surface $x^4 = P(z)$. It has the form of $Z_{e_i} \bar{Z}_{m_i} - Z_{m_i} \bar{Z}_{e_i}$ where e_i, m_i is a basis of electric and magnetic cycles (i.e. a basis of cycles which are symplectically normalized). For the particular case of the hexagon, $A_{\text{periods}} = |Z|^2$, where Z is defined in (3.1), see (4.1). A_{cutoff} is imposing the physical cutoff which requires that the AdS radial coordinate Y^+ should be larger than $1/\epsilon_c$. Here ϵ_c is a distance scale providing a UV (IR) cutoff in the Wilson loop (amplitude) interpretation.

In order to evaluate A_{cutoff} we can take $\Lambda = 0$ and replace the w surface by a simple surface with all the branch points at the origin. Our task is now to evaluate A_{cutoff} . In order to evaluate it we will need to use a couple of properties of the solutions discussed in section 2.4. Near each cusp we have a behavior which goes roughly like

$$Y_i^A \sim y_i^A \times \left(e^{2\text{Re}[w]}, \quad \text{or} \quad e^{2\text{Im}[w]}, \quad \text{or} \quad e^{-2\text{Re}[w]}, \quad \text{or} \quad e^{-2\text{Im}[w]} \right) \tag{A.2}$$

with a particular choice at each cusp (we have rotated the w plane so simplify these expressions). The position of the cusp on the boundary is determined by the null vector y_i ($y_i \cdot y_i = 0$). Recall that we had a basis of small solutions s_i , normalized so that $\det(s_i, s_{i+1}, s_{i+2}, s_{i+3}) = 1$. The behavior of the spacetime solution near the cusp i could

be found as $y_i^A = q_I^A s_i^T \Gamma^I s_{i+1}$. Which, together with the normalization condition on the s^I implies

$$y_i \cdot y_{i+2} = 1 \quad (\text{A.3})$$

Let us say that at cusp i we have $Y_i \sim y_i e^{2Re[w]}$. Then the spacetime cutoff has the form

$$Y^+ = \frac{1}{\epsilon_c} = y_i^+ e^{2Re[w]} \quad (\text{A.4})$$

which gives a line in the w plane, $2Re[w] = -\log \epsilon_c - \log y_i^+$. We have a similar relation on the cusp Y_{i+2}^+ , where the line is now at $2Re[w] = -(-\log[\epsilon_c] - \log y_{i+2}^+)$. We first imagine some reference lines at $2Re[w] = \pm \log \epsilon_c$ which are then displaced by small distances proportional to $\delta_i = -\log y_i^+$. It is convenient to relate the δ_i to the spacetime distances. This is done as follows. We know that $y_i \cdot y_{i+2} = 1$. At the same time we know that the spacetime distances can be expressed as $d_{i,i+2}^2 \sim \frac{y_i \cdot y_{i+2}}{y_i^+ y_{i+2}^+}$. This implies that

$$\delta_i + \delta_{i+2} = \ell_i \equiv \log d_{i,i+2}^2 \quad (\text{A.5})$$

where we used (A.3). This equation, together with $\delta_{i+n} = \delta_i$ can be used to solve for all the δ_i in terms of the logs of the nearby distances ℓ_i . Here it is important that n is not a multiple of four.

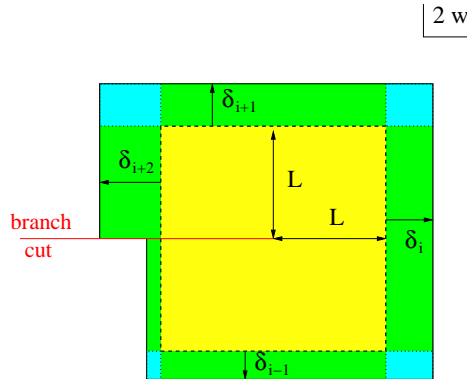


Fig. 18: Here we show the computation of A_{cutoff} . The w surface Σ_0 has a single branch point at the origin. We show only a portion of this surface. Here $L = -\log \epsilon_c$ and $\delta_i = -\log y_i^+$. The total area is obviously the sum of the areas of the various rectangles. Note that $L \gg \delta_i$ as we take the cutoff away.

We can then compute the area by summing the areas of various rectangles in fig. 18.

We get

$$\begin{aligned}
A_{\text{cutoff}} &= \frac{1}{2} \left[nL^2 + 2L \sum_i \delta_i + \sum_i \delta_i \delta_{i+1} \right] \\
A_{\text{cutoff}} &= A_{\text{div}} + A_{\text{BDS-like}} \\
A_{\text{div}} &= \frac{1}{2} \sum_i \left(-\log \epsilon_c + \frac{\delta_i + \delta_{i+2}}{2} \right)^2 = \frac{1}{8} \sum_i (\log(\epsilon_c^2 d_{i,i+2}))^2 \\
A_{\text{BDS-like}} &= -\frac{1}{4} \delta_i^2 - \frac{1}{4} \delta_i \delta_{i+2} + \frac{1}{2} \delta_i \delta_{i+1}
\end{aligned} \tag{A.6}$$

We can rewrite this as

$$\begin{aligned}
A_{\text{BDS-like}} &= -\frac{1}{8} \sum_{i=1}^n \left(\ell_i^2 + \sum_{k=0}^{2K} \ell_i \ell_{i+1+2k} (-1)^{k+1} \right), \quad \text{for } n = 4K + 2 \\
&= -\frac{1}{4} \sum_{i=1}^n \left(\ell_i^2 + \sum_{k=0}^{2K} \ell_i \ell_{i+1+2k} (-1)^{k+1} \right), \quad \text{for } n = 4K + 1, 4K + 3
\end{aligned} \tag{A.7}$$

Here A_{div} is the standard divergent term that is present for light-like Wilson loops or for amplitudes [46,47,48]. On the other hand $A_{\text{BDS-like}}$ is a finite term which obeys the anomalous Ward identities of broken conformal invariance [34]. An easy way to check this is to note that if we shift each log of a distance $\log d_{i,j}^2 \rightarrow \log d_{i,j}^2 + \epsilon_i + \epsilon_j$, then

$$\frac{dA_{\text{BDS-like}}}{d\epsilon_i} \Big|_{\epsilon=0} = \frac{dA_{\text{BDS}}}{d\epsilon_i} \Big|_{\epsilon=0} = \frac{1}{4} \log \frac{d_{i-1,i+1}^4}{d_{i,i+2}^2 d_{i,i-2}^2} \tag{A.8}$$

where A_{BDS} is the expression written in [35], which is the one loop result in the weak coupling expansion, except that here it comes with a different overall factor, due to the different value of the cusp anomalous dimension. When we act with the dual conformal generators we see that we need to add with these derivatives. Thus if we have the same derivatives as the BDS answer, then it obeys the same equations as the BDS answer. Note that if n is not a multiple of four we cannot make any cross ratios from the distances $d_{i,i+2}$. This implies that there is a unique solution of the anomalous ward identity which can be written only in terms of $d_{i,i+2}$. This unique solution is $A_{\text{BDS-like}}$.

In order to find the difference between $A_{\text{BDS}} - A_{\text{BDS-like}}$ we simply start with any non-nearby distance, $d_{i,j}$, appearing in A_{BDS} and we write it in terms of the unique cross ratio $c_{i,j}$ which involves $d_{i,j}$ and nearby distances $d_{i,i+2}$.

Thus, if one is interested in the remainder function, which is conventionally defined in terms of what we have to add to A_{BDS} to get the full answer, then it can be expressed as follows

$$\begin{aligned} -A &= -A_{\text{div}} - A_{\text{BDS}} + R \\ R &= -(A_{\text{BDS-like}} - A_{\text{BDS}}) - A_{\text{periods}} - A_{\text{free}} + \text{constant} \end{aligned} \tag{A.9}$$

where the constant is independent of the kinematics.

In the AdS_3 limit these formulas become the expressions for $n/2$ odd in [25] (Formula 5.8).

In this paper we are mostly interested in the case $n = 6$. In this case, the BDS ansatz reads¹⁴

$$A_{\text{BDS}} = \sum_{i=1}^6 \left[\frac{1}{4} \log \frac{x_{i,i+2}^2}{x_{i,i+3}^2} \log \frac{x_{i+1,i+3}^2}{x_{i,i+3}^2} - \frac{1}{16} \log^2 \frac{x_{i,i+3}^2}{x_{i+1,i+4}^2} + \frac{1}{8} Li_2 \left(1 - \frac{x_{i,i+2}^2 x_{i+3,i+5}^2}{x_{i,i+3}^2 x_{i+2,i+5}^2} \right) \right] \tag{A.10}$$

We find that

$$A_{\text{BDS}} - A_{\text{BDS-like}} = \sum_{i=1}^3 \left(\frac{1}{8} \log^2 u_i + \frac{1}{4} Li_2(1 - u_i) \right) \tag{A.11}$$

Hence, the remainder function is obtained by adding the above difference to the regularized area discussed in the body of the paper.

Appendix B. A new class of regular solutions

In the following we will consider a generalization of the regular polygon solutions considered in [25]. These are simple solutions for which the area can be evaluated directly. Thus, they provide special cases which can be compared to the general results we obtained above. We consider solutions that possess Z_n symmetry. In other words, we have

$$Y^A(z e^{i\frac{2\pi}{n}}, \bar{z} e^{-i\frac{2\pi}{n}}) = R_B^A Y^B(z, \bar{z}) \tag{B.1}$$

where R a rotation in space-time, $R^n = 1$. These solutions are associated to regular polygons. Using the expression (2.10) for the holomorphic function $P(z)$, this implies

$$P(z e^{i\frac{2\pi}{n}}) = e^{-4i\frac{2\pi}{n}} P(z) \tag{B.2}$$

¹⁴ Note that what we are calling A_{BDS} is minus the expression in [35] (up to a factor) because of the minus sign in (2.8).

The simplest holomorphic function satisfying this condition is a monic polynomial $P(z) = z^{n-4}$. For the case of AdS_3 we have n even. In the general case of AdS_5 , the simplest elementary solution would correspond to $P(z) = z$, which would correspond to a regular pentagon.

As seen in [49], it is convenient to use $(2, 2)$ signature to construct the pentagon because we can then choose all non-consecutive cusps to be spacelike separated. Furthermore, we will see that it can be actually embedded into AdS_4 , very much like the regular polygons studied in [25] could be embedded in AdS_3 .

We start by considering the embedding coordinates of AdS_5 in the case of $(2, 2)$ signature.

$$-Y_{-2}^2 - Y_{-1}^2 - Y_0^2 + Y_1^2 + Y_2^2 + Y_3^2 = -1 \quad (\text{B.3})$$

the restriction to AdS_4 corresponds to setting $Y_3 = 0$. Note that this is an AdS_4 space with two times, whose boundary has two time and one space directions. We can instead use ordinary AdS_5 Poincare coordinates, which correspond to $\frac{1}{z} = Y_{-2} + Y_3 = Y_{-2}$, $(t_1, t_2) = \frac{(Y_{-1}, Y_0)}{Y_{-2}}$ and $(x_1, x_2) = \frac{(Y_1, Y_2)}{Y_{-2}}$. The regular polygons to be considered in this appendix can be embedded into this AdS_4 , hence, they correspond to contours in the (x_1, x_2) plane and in the (t_1, t_2) plane, such that

$$x_1^2 + x_2^2 - t_1^2 - t_2^2 = 1 \quad (\text{B.4})$$

This is a surface inside $R^{2,2}$ with two time and one space directions. This surface is the boundary of an AdS_4 subspace of AdS_5 where the surface is residing. In addition, we require each segment to be light-like, so the lengths in the x -plane and t -plane coincide. Finally, we consider only polygons such that at each cusp the momentum transfer is space-like. This can be achieved by requiring that the angle between consecutive segments in the x -plane is larger than the angle in the t -plane. A prototypical example of such contour is the regular pentagon

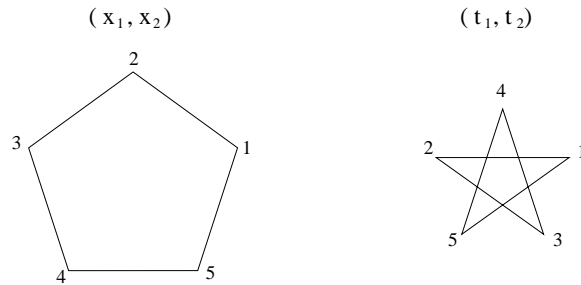


Fig. 19: Regular pentagon in $(2, 2)$ signature. The lengths of each segment in the x -plane and t -plane coincide and the angles are always smaller in the t -plane.

B.1. Strings on AdS_4

Next, let us briefly consider the reduction of strings on AdS_4 . In this case B_1 and B_2 are non trivial and we have v_1 and v_2 correspondingly. From now on, let us focus on the case of $(3, 1)$ signature and parametrize

$$v_1 = iP(z)^{1/2} \cos(\beta/2), \quad v_2 = P(z)^{1/2} \sin(\beta/2) \quad (\text{B.5})$$

where β is real. Later on, we will then continue to $(2, 2)$ signature by simply taking $\beta \rightarrow i\beta$. We would like to express the physical field β purely in terms of space-time quantities. For that, let us recall the following expressions

$$\partial^2 Y = \partial\alpha\partial Y + v^I B_I, \quad \bar{\partial}^2 Y = \bar{\partial}\alpha\bar{\partial} Y + \bar{v}^I B_I \quad (\text{B.6})$$

Viewing this as an expression for v^I, \bar{v}^I we can compute

$$-v^I \bar{v}^I = |P(z)| \cos \beta = e^\alpha \partial\alpha \bar{\partial}\alpha - \partial^2 Y \bar{\partial}^2 Y \quad (\text{B.7})$$

In addition, with a little bit of effort, one can show

$$e^\alpha |P(z)| \sin \beta = \epsilon_{abcde} Y^a \partial Y^b \bar{\partial} Y^c \partial^2 Y^d \bar{\partial}^2 Y^e \quad (\text{B.8})$$

From this relation we can immediately see that β is real and also that $\beta \rightarrow i\beta$ is the correct prescription in order to continue $(3, 1)$ signature into $(2, 2)$ signature.

B.2. Boundary conditions at zero

Let us now focus on the case of $(2, 2)$ signature. In that case, the equations of motion and Virasoro constraints imply the following equations for $\hat{\alpha} = \alpha - \frac{1}{2} \log |P(z)|$ and β

$$\partial\bar{\partial}\hat{\alpha} = e^{\hat{\alpha}} - e^{-\hat{\alpha}} \cosh \beta, \quad \partial\bar{\partial}\beta = e^{-\hat{\alpha}} \sinh \beta \quad (\text{B.9})$$

where we have written these equations in the w -plane, defined by $dw = P(z)^{1/4} dz$. As it can be seen, $\hat{\alpha}$ and β are massive fields that decay exponentially at infinity.

In order to understand the boundary conditions as we approach one of the zeros of $P(z)$, we use polar coordinates $z = \rho e^{i\varphi}, \bar{z} = e^{-i\varphi}$ and consider the expansion of a general solution around $\rho = 0$

$$Y_{-2} = 1 + \sum_{\ell=1} \Phi_{\ell}^{(-2)}(\varphi) \rho^{\ell}, \quad Y_i = \sum_{\ell=1} \Phi_{\ell}^{(i)}(\varphi) \rho^{\ell}, \quad i = -1, 0, 1, 2. \quad (\text{B.10})$$

By considering the equations of motion order by order in ρ , the functions $\Phi_\ell^{(i)}(\varphi)$ are determined, up to integration constants at each order. In addition, the requirement $Y^2 = -1$ and the Virasoro constraints impose some conditions on these integration constants. When considering the case of the regular pentagon, we have an additional constraint, coming from the Z_5 symmetry of the contours, see fig. 19. More precisely, we can introduce complex spacetime coordinates $X = Y_1 + iY_2$, $T = Y_{-1} + iY_0$ and we then require

$$X(ze^{i\frac{2\pi}{n}}, \bar{z}e^{-i\frac{2\pi}{n}}) = e^{i\frac{2\pi}{n}r_x} X(z, \bar{z}), \quad T(ze^{i\frac{2\pi}{n}}, \bar{z}e^{-i\frac{2\pi}{n}}) = e^{i\frac{2\pi}{n}r_t} T(z, \bar{z}) \quad (\text{B.11})$$

Where r_x and r_t are two integers which parametrize the spacetime Z_n rotation matrix. For the pentagon case, $n = 5$, $r_x = 1$ and $r_t = 2$, see fig. 19. Once all the constraints are worked out, we can compute the expansions of α and β around the origin. As expected, α is regular, while

$$\cosh \beta = \frac{e^\alpha \partial \alpha \bar{\partial} \alpha - \partial^2 Y \bar{\partial}^2 Y}{|\partial^2 Y \bar{\partial}^2 Y|} \approx \frac{1}{\rho} + \dots \quad (\text{B.12})$$

Hence β has a logarithmic divergence as we approach $\rho \rightarrow 0$. A similar argument for (3, 1) signature, shows that we should expect some winding in β as we approach the origin. Since $\cosh \beta \geq 1$ and $\cos \beta \leq 1$ it is reasonable to expect such behaviors for β from (B.12)¹⁵.

Hence we expect the regular pentagon in (2, 2) signature to correspond to two fields $\hat{\alpha}$ and β with logarithmic divergences at the origin and exponential decay at infinity. Furthermore, it is reasonable to assume that such solutions are rotationally symmetric. Namely $\hat{\alpha}$ and β are functions of $|w| = \rho$ only with the following boundary conditions.

$$\begin{aligned} \hat{\alpha}(\rho) &= -\frac{2}{5} \log \rho + c_\alpha + \dots, & \beta(\rho) &= -\frac{4}{5} \log \rho + c_\beta + \dots, & \rho &\rightarrow 0 \\ \hat{\alpha}(\rho) &\approx K_0(2\sqrt{2}\rho), & \beta(\rho) &\approx K_0(2\rho), & \rho &\rightarrow \infty \end{aligned} \quad (\text{B.13})$$

¹⁵ More precisely, the left hand side of (B.12) will have a general expansion of the form

$$[\cosh \beta \text{ or } \cos \beta] = \frac{e^\alpha \partial \alpha \bar{\partial} \alpha - \partial^2 Y \bar{\partial}^2 Y}{|\partial^2 Y \bar{\partial}^2 Y|} = \frac{c_1 + c_2 z + c_2^* z + \dots}{\rho}$$

For (2, 2) signature, as $\cosh \beta \geq 1$, we expect $c_1 \neq 0$. On the other hand, for (2, 2) signature, as $\cos \beta \leq 1$ we expect $c_1 = 0$ and $c_2 z + c_2^* z = \cos(\varphi + \gamma)$, resulting in non-trivial winding for β . The winding for β in (3, 1) signature is consistent with the assumption of β_{Dorn} as defined by [23], being regular everywhere. In [23] P is factorized in two polynomials $P(z) = v_+(z)v_-(z)$ and the relation between our β and the one used in [23] is $\beta_{\text{ours}} = \beta_{\text{Dorn}} - \frac{i}{2} \log \left(\frac{v_- \bar{v}_+}{v_+ \bar{v}_-} \right)$.

The constants c_α and c_β have to be chosen in such a way that the solutions decay at infinity. We find numerically that such solutions indeed exist and their exponential decaying is in perfect agreement with the expectations. Solving numerically the shooting problem, we find $c_\alpha \approx -0.28, c_\beta \approx -0.38$. These values are consistent with a crude version of the analysis of [50]¹⁶. Once the numerical solution is found, we can compute its regularized area. We find the approximate result

$$A_{\text{pentagon}} = 2 \int (e^{\hat{\alpha}} - 1) d^2 w \approx 1.18 \quad (\text{B.14})$$

with an estimated error of a few percent. Note that $\beta \rightarrow -\beta$ is a symmetry of the equations and we get another solution where $\beta \rightarrow -\frac{4}{5} \log \rho$ at the origin. These two pentagons differ by a spacetime parity operation¹⁷. For a more general polynomial we can choose either boundary condition, $\beta^\pm \rightarrow \pm \frac{4}{5} \log \rho$, at each zero of $P(z)$.

B.3. Other regular solutions

Now we can imagine that $P(z)$ has two zeros, in each of which β has boundary conditions β^\pm . As we bring the two zeros together there are two distinct situations:

1.- We bring together two zeros where the boundary conditions are β^+ and β^- . In this limit, we expect to recover the usual regular hexagon, which can be embedded into AdS_3 and for which $\beta = 0$. In terms of contours in $(2, 2)$ signature, its boundary looks like

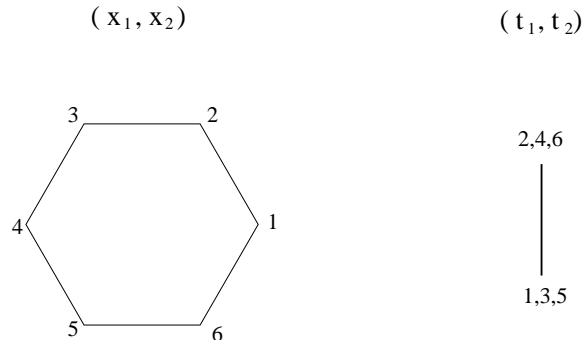


Fig. 20: Usual regular hexagon in $(2, 2)$ signature. As it can be embedded into AdS_3 , since one of the time coordinates vanishes identically. The cross ratios are $u_1 = u_2 = u_3 = 1$.

¹⁶ However, in [50] it was assumed that β is regular at $\rho \rightarrow 0$, while we assume a logarithmic divergence (B.13)r.

¹⁷ The fact that spacetime parity changes the sign of β can be seen from (B.8).

The regularized area corresponding to this hexagon was computed in [25], with the result

$$A_{\text{hexagon}}^{+-} = \frac{7}{12}\pi \quad (\text{B.15})$$

2.- We bring together two zeros where the boundary conditions are both β^+ (or both β^-). In this limit, we expect to recover a different regular hexagon, still with Z_6 symmetry, but which cannot be embedded in AdS_3 because $\beta \neq 0$. Furthermore, the field β corresponding to this solution has a logarithmic singularity at the origin. In terms of contours in $(2, 2)$ signature, its boundary looks like

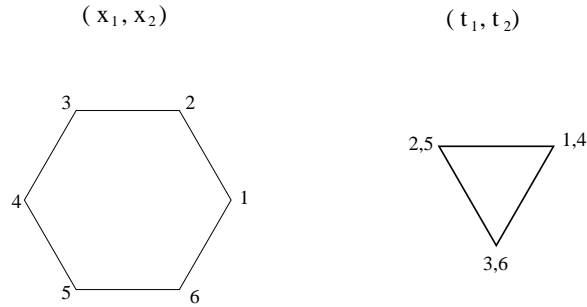


Fig. 21: Alternative regular hexagon in $(2, 2)$ signature. It still posses a Z_6 symmetry but cannot be embedded into AdS_3 . The cross ratios are $u_1 = u_2 = u_3 = \frac{1}{4}$.

In the w -plane we expect the following boundary conditions at the origin

$$\hat{\alpha}(\rho) = -\frac{2}{3}\log\rho + c_\alpha + \dots, \quad \beta(\rho) = -\frac{4}{3}\log\rho + c_\beta + \dots, \quad \rho \rightarrow 0 \quad (\text{B.16})$$

The condition for β is deduced by looking at (B.7) near the origin and demanding that the right hand side is approximately constant near the origin. Solving numerically the shooting problem and computing the approximate area, we find

$$A_{\text{hexagon}}^{++} \approx 2.85 \quad (\text{B.17})$$

The value of the cross-ratios is $u_i = 1$ for the first, usual, regular hexagon and $u_i = 1/4$ for the second kind of regular hexagon. It is difficult to compare these individual areas to the result of the integral equation due to possible overall additive constants. However we can compute the hexagon areas minus twice the pentagon area, which corresponds to

the difference in the regularized area when the two zeros are brought together from a very large distance. From our numerical estimates we find

$$A_{\text{hexagon}}^{+-} - 2A_{\text{pentagon}} \approx -0.52 \approx -\frac{\pi}{6}, \quad A_{\text{hexagon}}^{++} - 2A_{\text{pentagon}} \approx 0.50 \approx \frac{\pi}{6} \quad (\text{B.18})$$

The values $\pm\pi/6$ are the exact results obtained using the integral equation.

For a generic number of zeros of $P(z)$ we expect a similar situation. Given a polygon of n -sides, we can draw a regular polygon such that we need to perform a rotation by $\omega = e^{i2\pi p/n}$ in order to go from one cusp to the next one, with $p = 1, 2, \dots$. Hence, we will have a family of inequivalent polygons labeled by two integers (p_x, p_t) , drawing a regular polygon with p_x in the x -plane and with p_t in the t -plane, see (B.11). For instance, in the following figure we see different choices $p = 1, 2, 3, 4$ for $n = 9$.

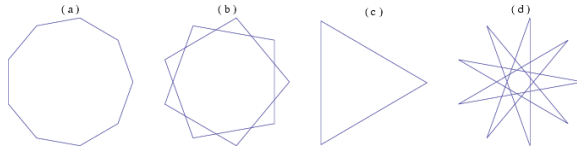


Fig. 22: Shape of different regular nonagons, with $p = 1, \dots, 4$ from left to right. The full polygon in $(2,2)$ signature is given by choosing a pair of these with $p_x < p_t$.

Furthermore, the requirement of space-like momentum transfer can be achieved by imposing $p_x < p_t \leq [\frac{n}{2}]$. Finally, let us mention that such polygons can be embedded into AdS_4 and the distance between adjacent cusps can be made light-like. Centering the above polygons at the origin we can rescale their relative size so that the segments in the x -plane and the t -plane have the same length. Then the pair of regular polygons produces a null-polygon in $R^{2,2}$.

It would be interesting to understand these solutions better. It is likely that they correspond to radially symmetric solutions. One could attempt to find the precise boundary conditions for β in each case.

Appendix C. On the appearance of poles in the TBA equation

Although in the initial large $|Z|$ region the $x_i[\zeta]$ had no zeroes or poles in ζ , they may appear at smaller $|Z|$. This is a familiar phenomenon in TBA-like equations [33,32]. Poles and zeroes appear in a very specific manner. Lets' start from a situation without poles or zeroes, and for simplicity consider some function $\mathcal{X}(\zeta)$, with a discontinuity $\mathcal{X}^+ =$

$\mathcal{X}^-(1 + \mathcal{Y})$ across a cut ℓ . In general, both the \mathcal{X}^+ , \mathcal{X}^- which define \mathcal{X} on the two sides will be nice analytic functions across the cut. \mathcal{X}^+ is supposed to have no zeroes or poles above the cut, but it may have either below the cut. It is easy to see it has to be a zero: \mathcal{X}^- and \mathcal{Y} are not supposed to have zeroes or poles there, all that can happen is that $1 + \mathcal{Y}$ is zero at some point ζ_0 .

As we vary the parameters in the integral equation, the point ζ_0 defined by $\mathcal{Y}[\zeta_0] = -1$ may move across the cut. In that case, we do not expect the zero of \mathcal{X}^+ to suddenly disappear, and a pole of \mathcal{X}^- to suddenly appear if we follow our solution continuously. That would happen, though, if we did not modify the integral equation. The reason is clear: the integral equation is of the form $\log \mathcal{X} = \dots + K_\ell * \log(1 + \mathcal{Y})$: the log has a singularity at ζ_0 , which we are passing across the cut.

The correct way to continuously follow a solution is to accept that \mathcal{X}^+ should have a zero at ζ_0 above the cut. The integral equation is easily modified to account for it, schematically as

$$\log \mathcal{X} = \dots + \log(\zeta - \zeta_0) + K_\ell * \log(1 + \mathcal{Y})$$

The extra term actually coincides with the difference between the convolution $K_\ell * \log(1 + \mathcal{Y})$ along paths just above and just below ζ_0 . Notice that the location of the zero is fixed by $\mathcal{Y}[\zeta_0] = -1$, in order for \mathcal{X}^- not to have the zero there.

The expression for the TBA free energy is similarly modified by the addition of a schematic term $Z/\zeta_0 + \bar{Z}\zeta_0$. In TBA these extra terms have the interpretation of an excitation added to the ground state. In our specific setup, the location of possible zeroes and poles is determined by equations of the form $u_i[\zeta_0] = \infty$ from the cuts $\tilde{\ell}_{i+1}$ and equations of the form $b_i[\zeta_0] = -\mu$ or $b_i[\zeta_0] = -\mu^{-1}$. It is easy to see that if, say, $b_i = -\mu$ then either $b_{i+1} = -\mu^{-1}$ or $b_{i-1} = -\mu^{-1}$, and one of the cross-ratios equals 1. The converse is also true. It seems possible that as we follow a path towards (3, 1) signature such phenomena will occur.

References

- [1] Douglas, J. “Solution of the problem of Plateau”. *Trans. Amer. Math. Soc.* **33** 263321 (1931).
- [2] N. Beisert, *Phys. Rept.* **405**, 1 (2005) [arXiv:hep-th/0407277].
- [3] I. Bena, J. Polchinski and R. Roiban, *Phys. Rev. D* **69**, 046002 (2004) [arXiv:hep-th/0305116].
- [4] L. F. Alday and J. M. Maldacena, *JHEP* **0706**, 064 (2007) [arXiv:0705.0303 [hep-th]].
- [5] G. Mandal, N. V. Suryanarayana and S. R. Wadia, *Phys. Lett. B* **543**, 81 (2002) [arXiv:hep-th/0206103].
- [6] G. Arutyunov, S. Frolov and M. Staudacher, *JHEP* **0410**, 016 (2004) [arXiv:hep-th/0406256].
- [7] V. A. Kazakov, A. Marshakov, J. A. Minahan and K. Zarembo, *JHEP* **0405**, 024 (2004) [arXiv:hep-th/0402207].
- [8] N. Beisert, B. Eden and M. Staudacher, *J. Stat. Mech.* **0701**, P021 (2007) [arXiv:hep-th/0610251].
- [9] D. Bombardelli, D. Fioravanti and R. Tateo, *J. Phys. A* **42**, 375401 (2009) [arXiv:0902.3930 [hep-th]].
- [10] N. Gromov, V. Kazakov, A. Kozak and P. Vieira, arXiv:0902.4458 [hep-th].
- [11] G. Arutyunov and S. Frolov, *JHEP* **0911**, 019 (2009) [arXiv:0907.2647 [hep-th]].
- [12] Z. Bern, L. J. Dixon, D. A. Kosower, R. Roiban, M. Spradlin, C. Vergu and A. Volovich, *Phys. Rev. D* **78**, 045007 (2008) [arXiv:0803.1465 [hep-th]].
- [13] J. M. Drummond, J. Henn, G. P. Korchemsky and E. Sokatchev, *Phys. Lett. B* **662**, 456 (2008) [arXiv:0712.4138 [hep-th]].
- [14] P. Dorey and R. Tateo, *J. Phys. A* **32**, L419 (1999) [arXiv:hep-th/9812211].
- [15] P. Dorey and R. Tateo, *Nucl. Phys. B* **563**, 573 (1999) [Erratum-ibid. *B* **603**, 581 (2001)] [arXiv:hep-th/9906219].
- [16] P. Dorey, C. Dunning and R. Tateo, *J. Phys. A* **40**, R205 (2007) [arXiv:hep-th/0703066].
- [17] K. Pohlmeyer, *Commun. Math. Phys.* **46**, 207 (1976).
- [18] H. J. De Vega and N. G. Sanchez, *Phys. Rev. D* **47**, 3394 (1993).
- [19] A. Jevicki, K. Jin, C. Kalousios and A. Volovich, *JHEP* **0803**, 032 (2008) [arXiv:0712.1193 [hep-th]].
- [20] M. Grigoriev and A. A. Tseytlin, *Int. J. Mod. Phys. A* **23**, 2107 (2008) [arXiv:0806.2623 [hep-th]].
- [21] J. L. Miramontes, *JHEP* **0810**, 087 (2008) [arXiv:0808.3365 [hep-th]].
- [22] A. Jevicki and K. Jin, *JHEP* **0906**, 064 (2009) [arXiv:0903.3389 [hep-th]].
- [23] H. Dorn, arXiv:0910.0934 [hep-th].
- [24] N. Arkani-Hamed, F. Cachazo, C. Cheung and J. Kaplan, arXiv:0903.2110 [hep-th].

- [25] L. F. Alday and J. Maldacena, arXiv:0904.0663 [hep-th].
- [26] L. F. Alday and J. Maldacena, arXiv:0903.4707 [hep-th].
- [27] A. Hodges, arXiv:0905.1473 [hep-th].
- [28] D. Gaiotto, G. W. Moore and A. Neitzke, arXiv:0807.4723 [hep-th].
- [29] D. Gaiotto, G. W. Moore and A. Neitzke, arXiv:0907.3987 [hep-th].
- [30] R. Koberle and J. A. Swieca, Phys. Lett. B **86**, 209 (1979).
- [31] A. B. Zamolodchikov, Phys. Lett. B **253**, 391 (1991).
- [32] V. V. Bazhanov, S. L. Lukyanov and A. B. Zamolodchikov, Nucl. Phys. B **489**, 487 (1997) [arXiv:hep-th/9607099].
- [33] P. Dorey and R. Tateo, Nucl. Phys. B **482**, 639 (1996) [arXiv:hep-th/9607167].
- [34] J. M. Drummond, J. Henn, G. P. Korchemsky and E. Sokatchev, arXiv:0712.1223 [hep-th].
- [35] Z. Bern, L. J. Dixon and V. A. Smirnov, Phys. Rev. D **72**, 085001 (2005) [arXiv:hep-th/0505205].
- [36] P. Fendley, Nucl. Phys. B **374**, 667 (1992) [arXiv:hep-th/9109021].
- [37] P. Fendley and K. A. Intriligator, Nucl. Phys. B **372**, 533 (1992) [arXiv:hep-th/9111014].
- [38] A. B. Zamolodchikov, Nucl. Phys. B **342**, 695 (1990).
- [39] A. N. Kirillov and N. Y. Reshetikhin, J. Phys. A **20**, 1565 (1987).
- [40] M. J. Martins, Phys. Rev. Lett. **67**, 419 (1991).
- [41] L. F. Alday and J. M. Maldacena, JHEP **0711**, 019 (2007) [arXiv:0708.0672 [hep-th]].
- [42] C. Anastasiou, A. Brandhuber, P. Heslop, V. V. Khoze, B. Spence and G. Travaglini, arXiv:0902.2245 [hep-th].
- [43] J. M. Drummond, J. Henn, G. P. Korchemsky and E. Sokatchev, arXiv:0803.1466 [hep-th].
- [44] A. Brandhuber, P. Heslop, V. V. Khoze and G. Travaglini, arXiv:0910.4898 [hep-th].
- [45] V. Del Duca, C. Duhr and V. A. Smirnov, arXiv:0911.5332 [hep-ph].
- [46] I. A. Korchemskaya and G. P. Korchemsky, Phys. Lett. B **287**, 169 (1992).
- [47] A. Bassetto, I. A. Korchemskaya, G. P. Korchemsky and G. Nardelli, Nucl. Phys. B **408**, 62 (1993) [arXiv:hep-ph/9303314].
- [48] Z. Bern, L. J. Dixon and V. A. Smirnov, Phys. Rev. D **72**, 085001 (2005) [arXiv:hep-th/0505205].
- [49] L. F. Alday and J. Maldacena, JHEP **0711**, 068 (2007) [arXiv:0710.1060 [hep-th]].
- [50] A. Jevicki and K. Jin, arXiv:0911.1107 [hep-th].